DNMI
DET NORSKE METEOROLOGISKE INSTITUTT
klima

# DOWNSLOPE WINDSTORMS AT OPPDAL, NORWAY LOCAL DESCRIPTION AND NUMERICAL SIMULATIONS

KNUT HARSTVEIT, LARS ANDRESEN AND KNUT HELGE MIDTBØ

REPORT NO. 23/95 KLIMA

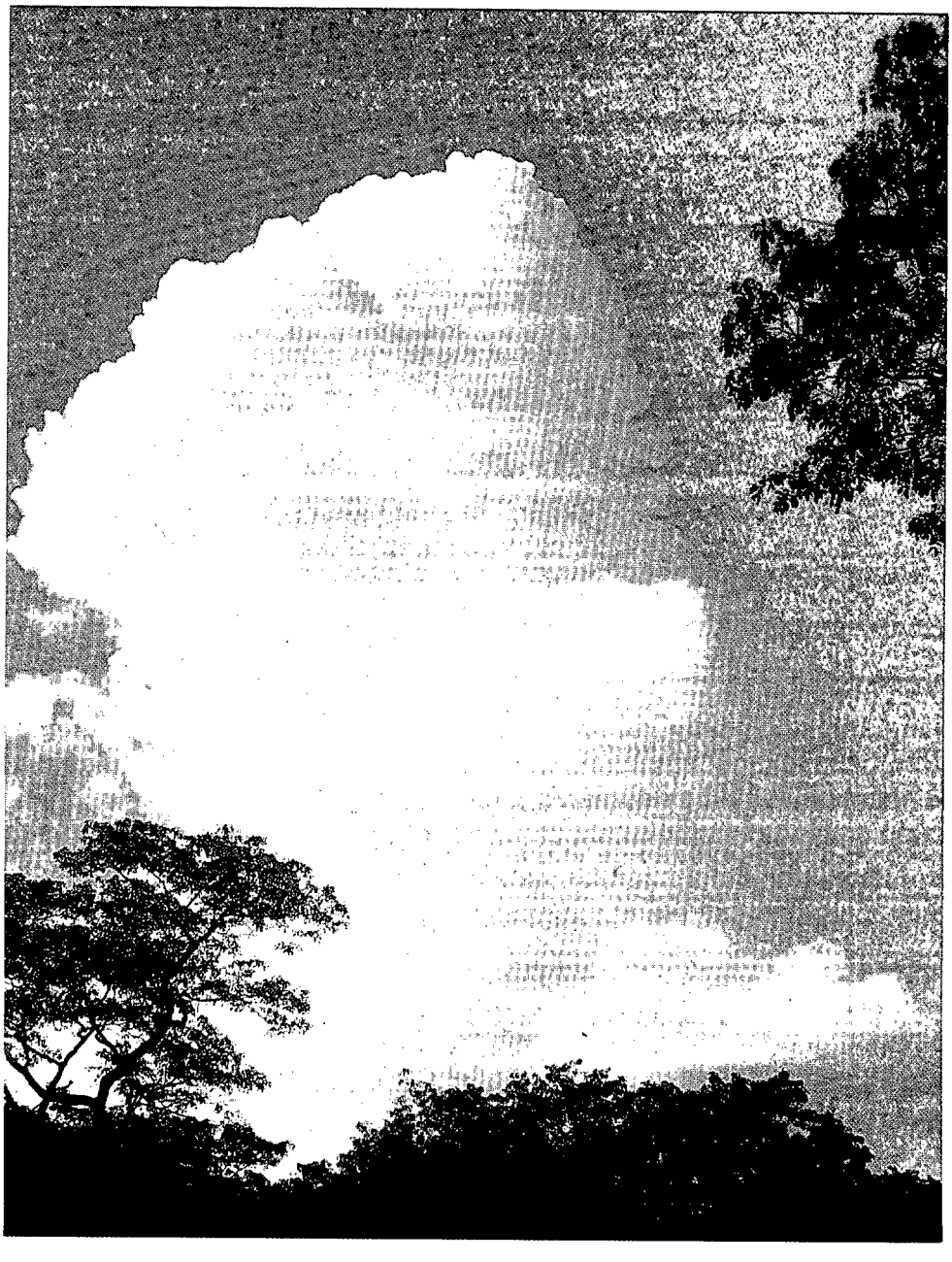

# DNMI-RAPPORT

ISBN 0805-9918

REPORT NO.
23/95 KLIMA

DATE
30.6.1995

NOWEGIAN METEOROLOGICAL INSTITUTE
P.O. Box 43 Blindern, N-0313 Oslo

TELEPHONE: +47 22 96 30 00

TITLE

## DOWNSLOPE WINDSTORMS AT OPPDAL, NORWAY LOCAL DESCRIPTION AND NUMERICAL SIMULATIONS

PREPARED BY

**KNUT HARSTVEIT, LARS ANDRESEN AND KNUT HELGE MIDTBØ**

ORDERED BY

**DNMI - CLIMATOLOGY DIVISION AND RESEARCH DIVISION**

SUMMARY

Damage on several houses and factory buildings due to strong winds were reported within limited areas at the winter sport village, Oppdal (62°36'N,9°42'E; 550 m a.s.l.) in Sør-Trøndelag, at the northern side of the mountain crest Breheimen-Dovre-Sylene on the dates 31.3. and 8.12.1994, 18.1., 20.1. and 31.1.1995. In all the situations a partly occluded front system and a strong southerly wind field approached the southern part of Norway from southwest. Observations from weather stations show low wind speeds at the lower areas uphill, accelerating up to the crest, and even stronger winds downhill.

The air stream is modified by the complex terrain. In **PART I** this is discussed by analysing the lifting condensation level at different weather stations downstream. It seems reasonable that strong wind is blowing over and around the local mountains Ålmanberget (1342 m a.s.l.) and Våtåhaugen (965 m a.s.l.), resulting in a cork-screw vortex in or near the Oppdal village. The conditions for such wind situations to occur is shown and a storm risk analysis is given. In **PART II** the five windstorms are simulated by using the operational mesoscale model at the Norwegian Meteorological Institute (LAM50S). The analysis shows a tilting mountain wave with a wind maximum over Oppdal in all the situations. This may be explained by reflection of gravity waves in the tropospere caused by a stable layer near the mountain top level.

SIGNATURE

Knut Harstveit

Knut Harstveit
SENIOR SCIENTIST

Bjørn Aune

Bjørn Aune
HEAD OF DIVISION

# Part I. Surface observations and local effects

## Table of contents



Acknowledgement

We thank Ingebrigt Bjerke, journalist in the newspaper Opdalingen, for mapping damages at Oppdal and searching for earlier storms in the newspaper archives.

# 1. Introduction

Damages due to strong wind were reported within limited areas at the winter sport village, Oppdal in Trøndelag, central Norway (62°36' N, 9°42' E; 550 masl., Fig. 1), on the days 31.03.94 (a), 08.12.94 (b), 18.01.95 (c), 20.01.95 (d) and 31.01.95 (e). Building damages at other places were untypical in these situations. Some damages were made 10 - 15 km west of Oppdal in situation (c), while very strong southerly wind were blowing at the Western part of the country causing sporadic damages in situation (e).

# 2. Damage description

According to the local press, Oppdalingen, about 50 building damages were reported at the centre of the village 31.03.94. Among which, the dairy roof was seriously damaged, and a bus garage, and a 400 $m^2$ storehouse were smashed to pieces. Local people living near the damaged area reported a strong roar for several hours. The area effected was about 2 km long and 1 km broad, with a long axis from SE to NW (Fig.2). 9 km northeast of the damaged area, a normal storm situation without damages were reported, and, as near as the skilifts, 3 - 4 km to northwest, almost no wind at all occurred.

Serious damages at approximately the same area were also reported through the situations (b) and (d). Reports given by interviewes from local observers, estimate the wind direction to SE in situation (a) and (d), while it was rather difficult to give a straight wind direction in situation (b).

The storms of 18. and 31. January, 1995, made corresponding damages 1 - 5 km east and northeast of the village centre, with a more eastern damage area during the last situation (Fig.2). The local wind direction were reported southerly to southwesterly.

Unfortunately, no wind records are available from the damaged area. However, the many serious damages indicate wind gusts above 60 m/s for all 5 situations.

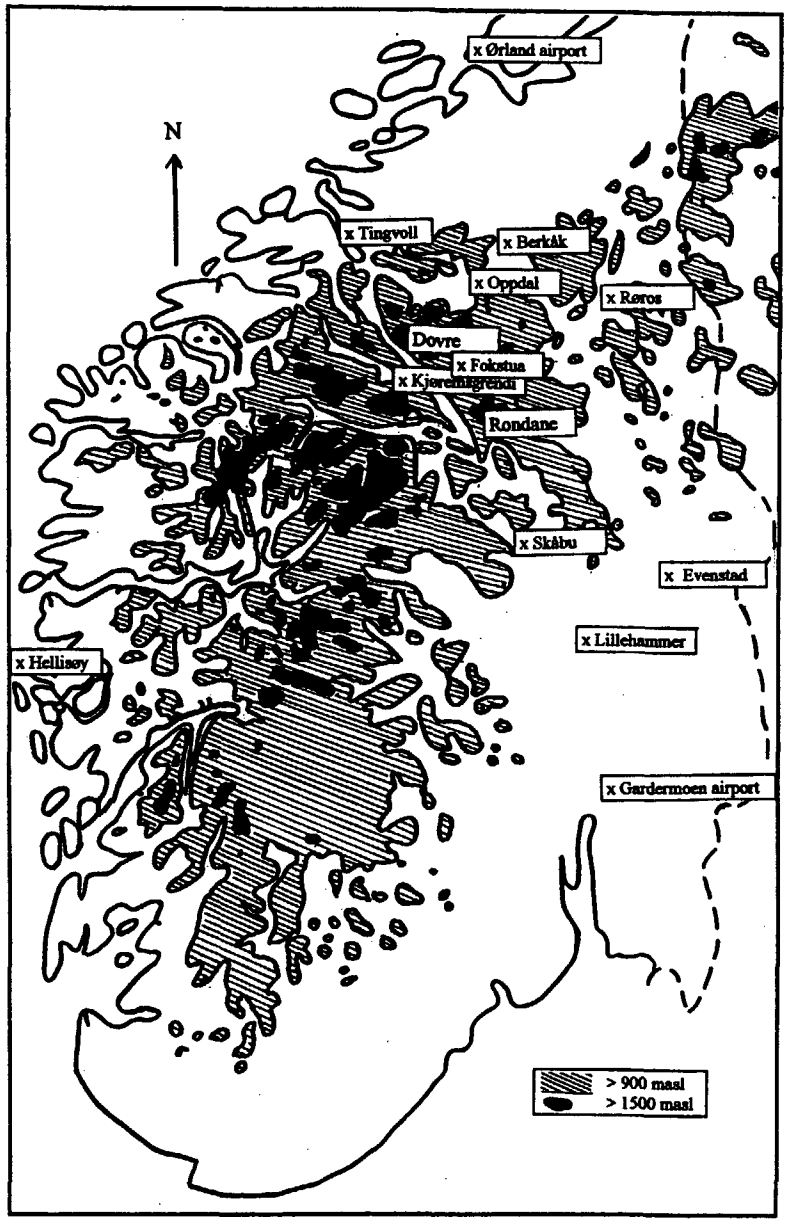


**Fig. 1a** *Map of Southern Norway at a scale of 1:4mill.*

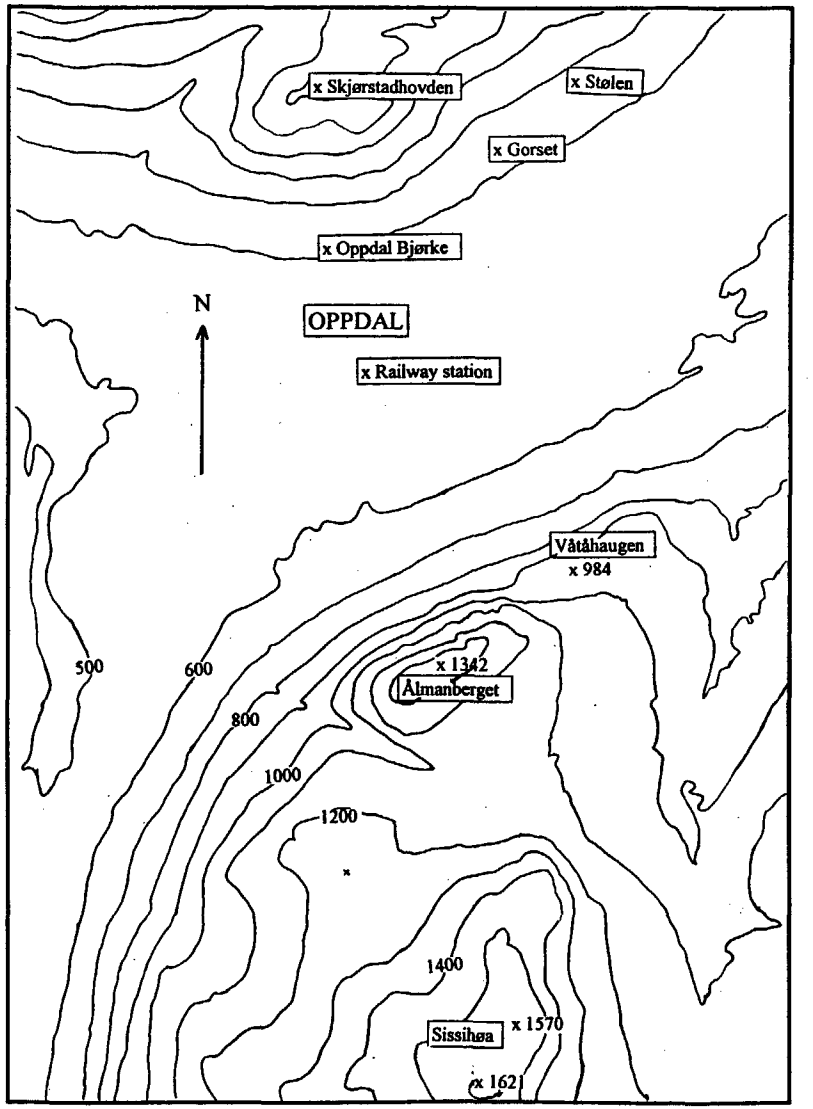


**Fig. 1b** *Map of the Oppdal area at a scale of 1:70 000*

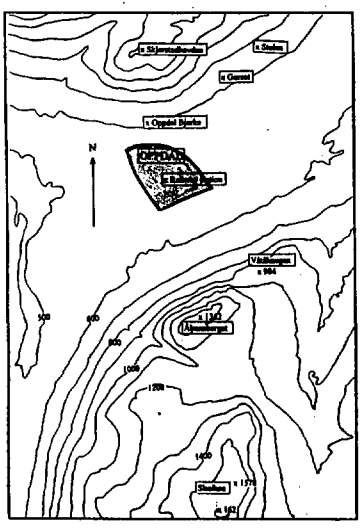

a) 31.03.94

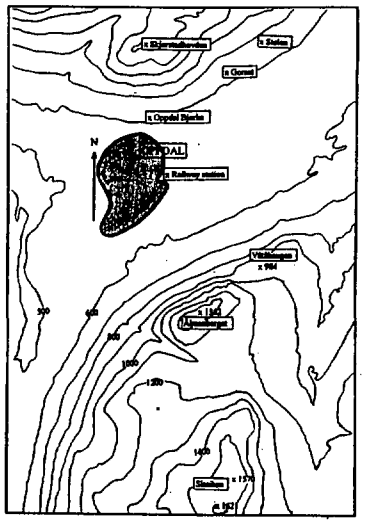

b) 8.12.94

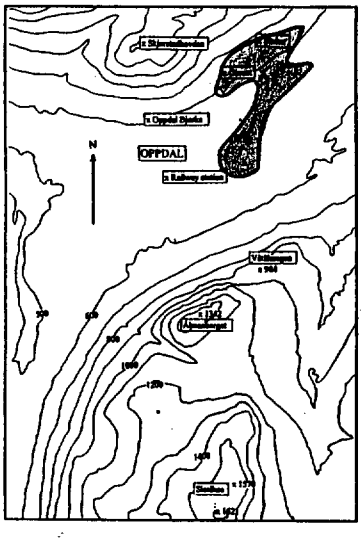

c) 18.01.95

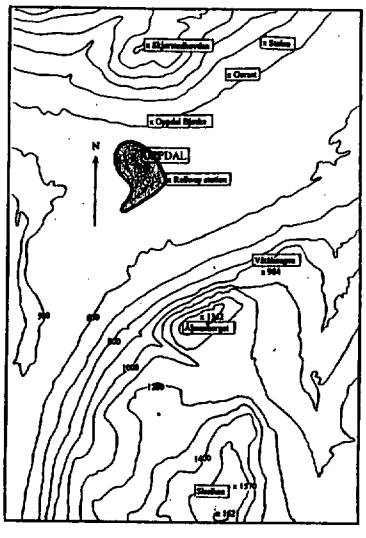

d) 20.01.95

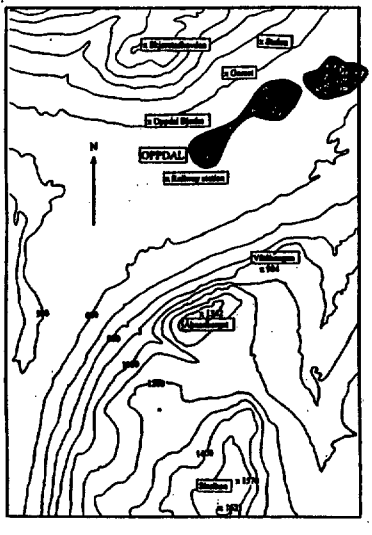

e) 31.01.95

**Fig. 2.**
*Map of damage (shaded area) at Oppdal during the five downslope windstorm situations in 1994/95.*

# 3. Weather data

All 5 situations occur when southerly wind fields followed by occluded fronts is penetrating the country, see part II for a further discussion. Surface observations from 9 anemometer stations within an area including Gardermoen - Røros - Ørland - Finse gave average values of 148, 142, 148, 144 and 157° for the five storm situations. From the numerical weather analysis we find wind directions at the top of the surface layer at the Oppdal region of 170, 170, 180, 170 and 200° (see part II). A backing of the surface wind of 20 - 40° is rather consistent with frictional drag. Further on, the more southwesterly wind direction of the situation (e) is found in the numerical model results as well as in the observations.

Table 1 shows observations of maximum potential temperature, and maximum wind speed at three sites at the uphill side, and three sites at the downhill side. Also given are data from mountain valleys near the large-scale crest, but at the uphill side of the watershed (Røros, Kjøremsgrendi, and Fokstua).

**Table 1**

*Maximum potential temperature, Txp (°C), and maximum wind speed, Fx (m/s), at different stations uphill, U, downhill, D, and at mountain valleys, M, for the five storm situations at Oppdal. The stations are located in Fig. 1.*

| Station | | masl | a Txp | b Txp | c Txp | d Txp | e Txp | Mean Txp |
|---|---|---|---|---|---|---|---|---|
| Gardermoen airp | U | 202 | 6.5 | 5.5 | 3.2 | 1.9 | -3.5 | 2.7 |
| Lillehammer | U | 241 | 7.6 | 5.6 | 3.8 | 1.9 | -3.2 | 3.1 |
| Evenstad | U | 255 | 6.5 | 4.7 | 4.5 | 2.9 | -6.5 | 2.4 |
| Uphill | U | 233 | 6.8 | 5.2 | 3.8 | 2.2 | -4.4 | 2.7 |
| Kjøremsgrendi | M | 626 | 8.2 | 7.8 | 7.2 | 3.3 | -0.7 | 5.2 |
| Fokstua | M | 972 | 9.8 | 8.9 | 6.7 | 4.3 | 1.8 | 6.3 |
| Røros | M | 628 | 10.2 | 9.2 | 7.2 | 3.2 | -0.2 | 5.9 |
| Mountain vly. | M | 742 | 9.4 | 8.6 | 7.0 | 3.6 | 0.3 | 5.8 |
| Berkåk | D | 475 | 10.7 | 6.9 | 7.7 | 3.5 | 1.2 | 6.0 |
| Tingvoll | D | 69 | 12.9 | 10.4 | 10.2 | 7.0 | 3.7 | 8.8 |
| Oppdal | D | 668 | 11.5 | 8.4 | 8.9 | 4.9 | 2.9 | 7.4 |
| Downhill | D | 404 | 11.7 | 8.6 | 8.9 | 5.1 | 2.6 | 7.4 |
| Mean, D-U | | | 4.8 | 3.3 | 5.1 | 2.9 | 7.0 | 4.6 |

| Station | | masl | a Fx | b Fx | c Fx | d Fx | e Fx | Mean Fx |
|---|---|---|---|---|---|---|---|---|
| Gardermoen airp | U | 202 | 6 | 9 | 6 | 9 | 8 | 7.6 |
| Lillehammer | U | 241 | 3 | 8 | 6 | 7 | 7 | 6.2 |
| Skåbu | U | 865 | 12 | 5 | 3 | 12 | 12 | 8.8 |
| Uphill | U | 436 | 7.2 | 7.3 | 4.9 | 9.4 | 9.0 | 7.6 |
| Kjøremsgrendi | M | 626 | 12 | 12 | 19 | 19 | 19 | 16.2 |
| Fokstua | M | 972 | 21 | 25 | 25 | 23 | 26 | 24.0 |
| Røros airport | M | 628 | 13 | 13 | 16 | 16 | 22 | 16.0 |
| Mountain vly. | M | 742 | 15.3 | 16.7 | 20.0 | 19.3 | 22.3 | 18.7 |
| Berkåk | D | 475 | 19 | 15 | 23 | 23 | 27 | 21.3 |
| Tingvoll | D | 69 | 23 | 23 | 19 | 27 | 23 | 22.7 |
| Ørland airport | D | 9 | 20 | 17 | 21 | 22 | 17 | 19.4 |
| Downhill | D | 184 | 20.6 | 18.3 | 20.9 | 23.7 | 22.3 | 21.2 |
| Mean, D/U | | | 2.9 | 2.5 | 4.3 | 2.5 | 2.5 | 2.9 |

The observations show low wind speed at the lower areas upstream the crest, while accelerating up to the crest, and even stronger wind is transported downhill. The potential temperature is higher in the mounatin region than at the upstream stations, but even higher at the downstream sites. All situations have stable stratification upstream, consistent with the picture from part II.

During the storm situations, the air upstream is saturated some hundred meters above sea level, for instance at Skåbu (865 masl). This indicate that the lifting condensation level, LCL, calculated from observations at certain points downstream, could be an interesting parameter in the discussion of which mountain area that has been crossed.

Table 2 shows the lifting condensation level, LCL, calculated from observed temperature and relative humidity by lifting the air mass adiabatically. The first four situations are all characterised by rather low LCL (1000 masl) at Oppdal, and near the same values at Berkåk, while higher values (1550 - 1800 masl) are found at Tingvoll. This indicates that the air at Berkåk and Oppdal probably blows over the lower mountains east of Rondane and Dovre, while the air at Tingvoll blows over the higher parts of the mountain chain.

**Table 2**
*Lifting condensation level, LCL (masl) at three downhill stations at the closest observational time to the wind maximum during the five storms at Oppdal 1994/95.*

| Station | 31.03.94 | 08.12.94 | 18.01.95 | 20.01.95 | 31.01.95 | M |
|---|---|---|---|---|---|---|
| Tingvoll, T | 1600 | 1760 | 1550 | 1760 | 1020 | 1538 |
| Berkåk, B | 960 | 890 | 1040 | 930 | 950 | 954 |
| Oppdal, O | 1040 | 980 | 1070 | 910 | 1300 | 1060 |
| T-O | 560 | 780 | 480 | 850 | -280 | 478 |
| O-B | 80 | 90 | 30 | -20 | 350 | 106 |

Situation (e) differs from the others. First, Oppdal has higher LCL than Berkåk. This is consistent with the more southwesterly wind field, giving more wind above the higher mountains south of Oppdal, while the wind at Berkåk still has passed the lower mountains. Second, the LCL value at Tingvoll is remarkably low. This indicates that the air has not passed the high mountains south and southeast of the station. Moist air from southwest has crossed lower mountains and made the LCL higher.

To conclude, in damage storm situations at Oppdal, the air seems to have been deflected eastward around Rondane and Dovre in southerly wind fields, while the air mostly passes the higher mountains when the wind field turns towards southsouthwest.

## 4. Local respons. Air stream reorganisation.

Surface observations as well as results from a hydrostatic numerical model (part II) show that strong wind is blowing downhill at the scale of 200 km. From part II we find a smoothed height of 1500 masl of the Oppdal area, which is close to the local mountain tops surrounding Oppdal. The average wind speed is modelled to some 35-40 m/s, 250 m above the smoothed surface, some less in situation (a), and slightly higher in situation (e). This is probably a better

estimate for the wind speed near the mountain tops than the wind speed at the smoothed surface which is reduced due to surface friction. From the model, the wind direction above Oppdal varied through 170 - 180° through the first four situations, and situtation (e) being more southwesterly than the others (200°).

Using higher model resolution (10 km grid, see part II), a more complicated wave pattern is found. It should, however, be read with care due to increasing nonhydrostatic effects. Zones of high wave energy due to wave breaking (for instance), and channelling/deflection of the air due to mountain massives represented by the actual scale could be found by doing analysis of increasing resolution using nonhydrostatic models. However, even a scale of a few hundreds of meter smoothes the steep mountains, Ålmanberget (1342 masl) and Våtåhaugen (965 masl), 3 km south of the damages area.

The edge of Ålmanberget is very sharp, the slope steepens from 0 to 45° over a horizontal distance of less than 100 m. For wind speed of 30 m/s, 100 m is covered in 3.5 seconds. Even for very stratified situations, the time scale of the gravity waves, $T=N^{-1}$, where N is the Vaisala-Brunt frequency, is at least one magnitude of order higher. This is much to short to give significant influence of the gravity waves near the cliff. To a first order of approximation, we may consider that the fast moving air at the edge behaves like neutral atmosphere at a corresponding surface. Such air stream separates at the edge in three dimensions (3D separation). The strong southerly wind passes above Ålmanberget, and it is also deflected around the mountain. The fast motion above the mountain near the edge make the wind separated from the ground and a local depression near the edge occure. The wind deflected around tries to fill up the depression, and a strong horizontal vortex probably occur.

The mountain Ålmanberget is an approximately 1100 m wide ridge at the 1300 m level, very steep at the downstream side, and with sharp corners at the southwestern and northeastern side. At first glance, the mountain looks like an ideal shaped body, a so-called $\cos^2(\alpha_1,\alpha_2,\alpha_L)$ mountain, where the angels $\alpha_1$ and $\alpha_2$ characterise the slopes accross and along the mountain ridge. The angel between the wind direction and the normal to the ridge is given by $\alpha_L$. Such a body is tested in wind tunnel as well as modelled by a numerical model of neutral stratified flow where also the turbulent wind shear (turbulent Reynold stresses) are taken into account, using a $(k,\varepsilon)$ modell (Eidsvik et. al, 1994). The wind tunnel results and the numerical results were very similar, giving wind separation at approximately the same area. For a steep body ($\alpha_1$=50°, $\alpha_2$,=25°, $\alpha_L$=0°), the wind was reattatched at a distance of 3 - 4 montain heights downstream of the mountain. The air was deflected into the separated area from outside, and mixed with the air above, and two small cork-screw vortexes could be seen downstream, one at each side of the body. Turning the ridge, $\alpha_L$=45°, one strong vortex and a much lesser separation area could be seen (Fig. 3). This situation transports strong wind down to the surface at the leeward side of the mountain. For southeasterly wind (150°), $\alpha_L$=0° at Oppdal, turning to $\alpha_L$=45° for south-soutwesterly wind (200°).

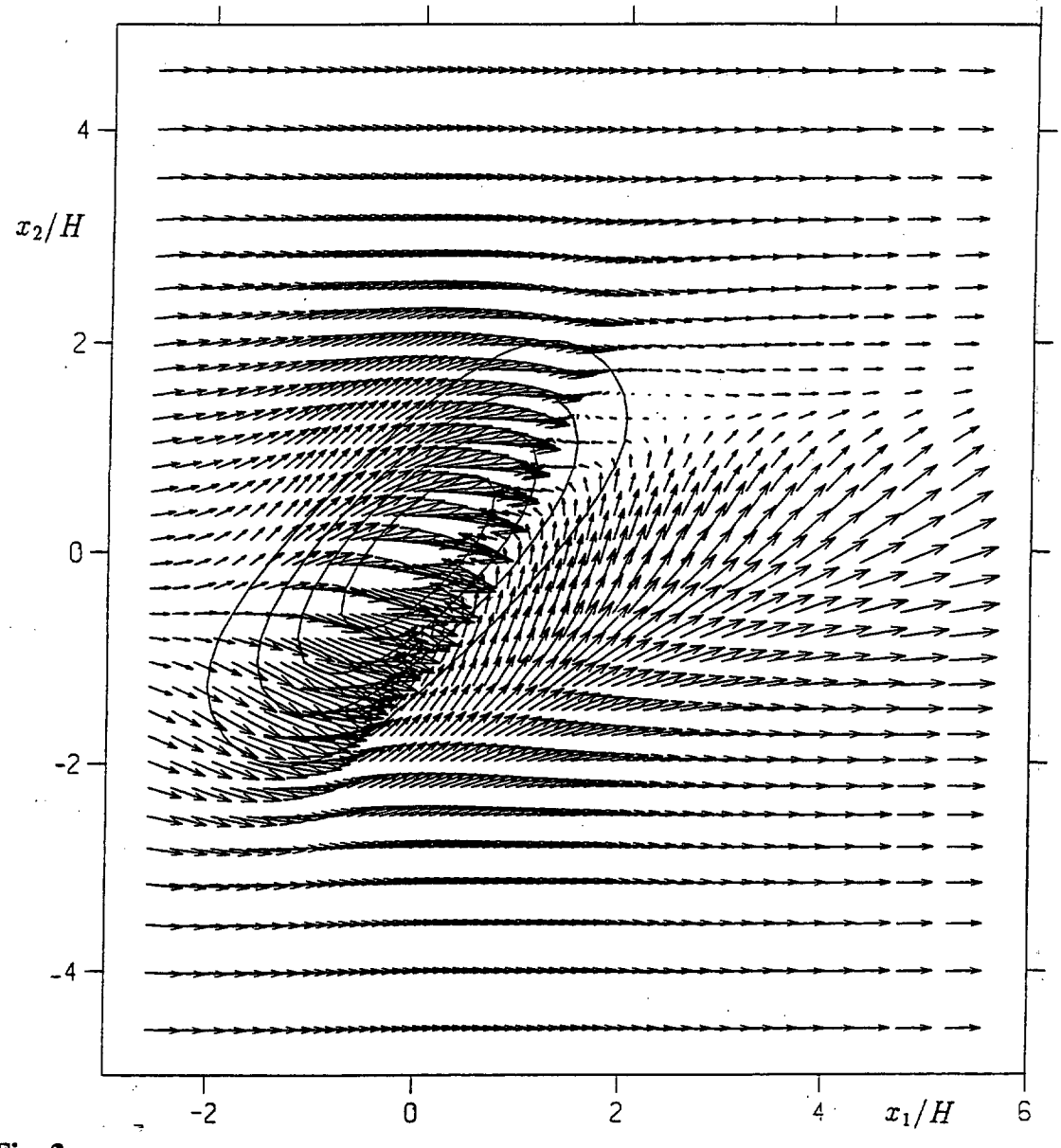


**Fig. 3**
*Numerical prediction of the flow pattern over a steep three-dimensional ridge for an angle of 45° between the ridge and the air flow. After Eidsvik et. all (1994).*

Jenkins et. al (1981) made air craft observations of such a vortex near a Scottish island, when strong wind passes a steep and asymmetric cliff. Very strong vertical wind speed were reported. Such a vortex can transport high wind speeds from the mountains down to Oppdal, and probably create stronger surface gusts than the high level wind speed. Many observations near Norwegian cliffs and small-scale moutain ridges indicate such vortexes. A number of serious damages from the storm of January 1., 1992 were located at such places (Andresen and Harstveit, 1993). Measurements from Fræna (62°57'N, 07°07'E) gave 20% stronger wind gusts at the downstream side, near the end of a steep ridge, related to wind at an open reference area, probably coarsed by a horizonal vortex. The situation occured when strong westerly wind was crossing the ridge at an angle, $\alpha_L$=30°, and the local wind direction turned 45°. The site was chosen due to several serious damages at a farm during the strong westerly storms in 1988 - 1992.

Looking at the differences between Ålmanberget and the ideal shaped body, we see that the downslope area is steeper than the upslope, and that the upstream area is situated at a higher level than the downslope area. Surface jets at both sides of the N - S running ridge upstream of Ålmanberget (Sissihøa and mountains further south) during large scale southeasterly and southerly wind (150 - 200°) probably occure. Channelled, southerly wind starts separating at the edge southwest of Ålmanberget. The result is a large scale vortex which turns the wind to southwest and west at Oppdal, a picture consistent with the observations at Oppdal. Fig. 4 shows that westerly wind direction is the most frequent one at Oppdal - Bjørke. However, this wind obviously occurs during at least two weather situations. In addition to the "true" westerly wind, the frequent wind direction is westerly and southwesterly also in situations when southerly and southeasterly winds dominate in the area. Observations from the short observational period (Dec 1992 - May 1993) at the railway station gave 77% wind in the sector 200 - 250° in situations when southerly and southeasterly winds dominate in the area.

It seems to be small chances for southeasterly to southerly wind at Oppdal, even for high wind speed in the area. However, analysis show that such wind is strong when it occure. In the period discussed, 1977-1992, only 4 cases of gale (8B) is observed at Oppdal - Bjørke at one of the three observational daily termins, and the wind direction is then given as 150, 180, 200, and 210°.

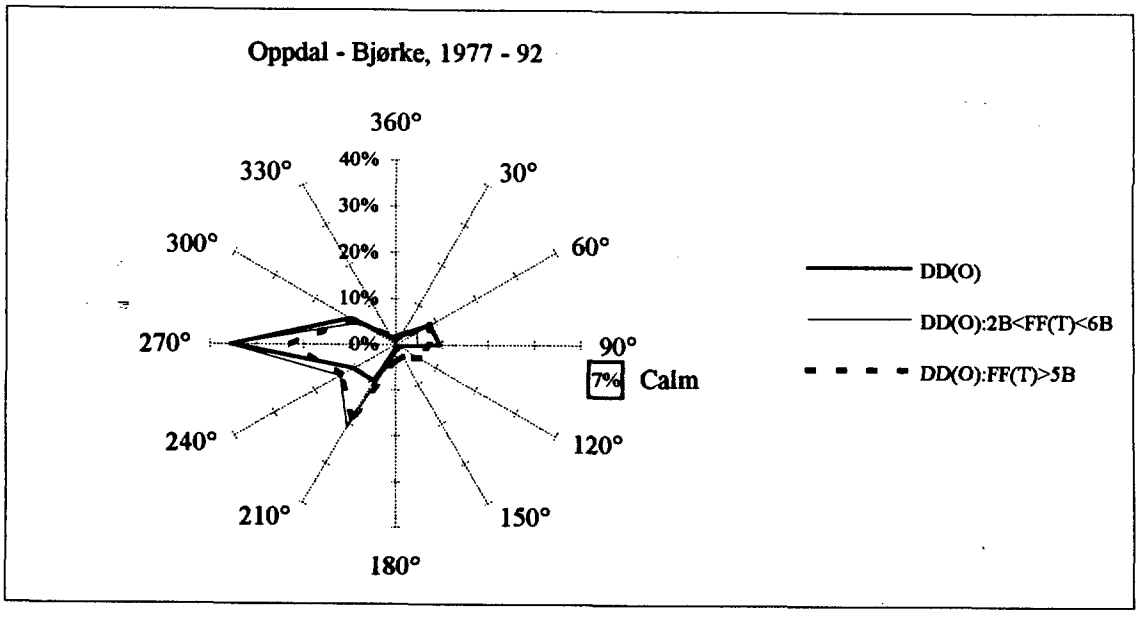


**Fig. 4.**
*Wind direction distribution, DD, at Oppdal - Bjørke, (O), covering all observations, compared to the observations given when southeasterly to southerly wind (140 - 200°) is observed at Tingvoll (T), for two Beaufort groupes at Tingvoll.*

At the upper part of the valley Ålmdalen, east of the ridge, southeasterly to southerly wind is probably channelled to 160 - 170°. This low level jet blows out over Våtåhaugen and the slope is steep enough for wind separation, but hardly for resirculation at lower levels. The

result is a strong wind shear and strong wind at 1000 m level out from Våtåhaugen. The dangerous situation probably occurs when this low level jet is deflected into the vortex behind Ålmanberget, feeding it with kinetic energy. The vortex (suggested in Fig. 5) trails out towards the centre of the village during wind at 1500 m level from SSE (160 - 170°), and to the east of the centre when the wind turns to S, and espescially for SSW (190 - 200°). In fact, the damage map is very consistent with the wind direction given by the operational model in these five situations.

## 5. Storm risk analysis at Oppdal

Five storm situations has coarsed damages at Oppdal during 10 months (31.03.94 - 31.01.95). These five wind storms may be described by surface observations at a few indicator stations. Looking at observations at the weather stations, it seems reasonable to use three indicators: Berkåk, Tingvoll and Hellisøy lighthouse. Berkåk and Tingvoll are both stations at the downslope area, 30 - 70 km from Oppdal. Both of them report near gale (7B) to storm (10B) with a typical maximum value of strong gale in each of the five situations. Further on, the stations usually observe strong wind during southerly wind fields. However, the wind are only estimated by the observer at the stations. Hellisøy lighthouse is taken into consideration because this station is a good indicator of the strength of incoming southerly wind fields. The weather station at Oppdal, Oppdal - Myrhaugen is a somewhat sheltered station at a valley side, 9 km northeast of the centre of Oppdal, and should not be used as an indicator of the wind at the centre. Other stations at Oppdal do not cover these storms.

Table 3 show that maximum wind speed of each of the three indicator stations has an average Beaufort value of 9.0B, and that the wind force at least has been 9B at either Berkåk or Tingvoll during the five storm situations at Oppdal. Using the whole common observation period for the three stations, 1973 - 1995, we find 3 or 4 storms in addition to the situations described, which have the criteria given, and further 3, which lies slightly below the criterion (8.7B). The table shows that it has been only one situation in the period 1973 - 1981, but several situations since 1982. However, the 10 month period March 1994 - January 1995 have a distinct overrepresentation of the storm index situations.

By inspecting local press for the nearest days after the situations mentioned in Table 3, we find that the storms of 10.03.82, 22.03.86, and 16.10.87, have been reported as storm situations with some building damages (roofs) and wood damages. However, the damages seem to have been lees severe than in the situations of 1994/95. The observations from Oppdal - Bjørke report maximum wind at 8B, 8B, and 7B for those 3 situations. Besides, some damages were described in the newspaper at 14.10.87. The damage probably has been made 8.10. and/or 11.10.87, two episodes with storm index 8.0B, and maximum wind force at Oppdal - Bjørke of 6B and 8B. For the situations 31.12.76, 27.11.84, 18.02.89, and 02.01.91 no damage was reported (Oppdal - Bjørke: 8B, 6B, 6B, and 6B). To conclude, it seems that the damages of 1994/95 are even more seldom than indicated from Table 3. This may be due to atmospheric conditions causing stronger wind from gravity waves or more unfavourable wind directions.

**Table 3**

*Storm index given as average of the maximum Beaufort value observed at three index stations in the five storms at Oppdal 1994/95. Also given is the other 7 southerly storms of the period from 1973 to May 1995 which has storm index corresponding to strong gale (9B) or more.*

| | Hellisøy | Tingvol | Berkåk | Mean |
|---|---|---|---|---|
| 31.01.95 | 12B | 9B | 10B | 10.3B |
| 20.01.95 | 9B | 10B | 9B | 9.3B |
| 31.03.94 | 10B | 9B | 8B | 9.0B |
| 08.12.94 | 11B | 9B | 7B | 9.0B |
| 18.01.95 | 10B | 8B | 9B | 9.0B |
| 16.10.87 | 11B | 9B | 9B | 9.7B |
| 31.12.76 | 10B | 9B | 9B | 9.3B |
| 02.01.91 | 10B | 9B | 9B | 9.3B |
| 10.03.82 | 10B | 9B | x | 9B |
| 27.11.84 | 10B | 7B | 9B | 8.7B |
| 22.03.86 | 10B | 7B | 9B | 8.7B |
| 18.02.89 | 9B | 8B | 9B | 8.7B |

x (10.03.82 probably has 9B storm index, but observation from Berkåk is missing)

**Table 4**

*Lifting condensation level, LCL (masl) at three downhill stations at the closest observational time to the wind maximum during the ten southerly storms, 1973-95.*

| Station | 31.03.94 | 08.12.94 | 18.01.95 | 20.01.95 | 31.01.95 | M |
|---|---|---|---|---|---|---|
| Tingvoll, T | 1600 | 1760 | 1550 | 1760 | 1020 | 1538 |
| Berkåk, B | 960 | 890 | 1040 | 930 | 950 | 954 |
| Oppdal, O | 1040 | 980 | 1070 | 910 | 1300 | 1060 |
| T-O | 560 | 780 | 480 | 850 | -280 | 478 |
| O-B | 80 | 90 | 30 | -20 | 350 | 106 |

| Station | 31.12.76 | 27.11.84 | 22.03.86 | 16.10.87 | 18.02.89 | 02.01.91 | M |
|---|---|---|---|---|---|---|---|
| Tingvoll | 1730 | 2260 | 1520 | 2000 | 1260 | 1780 | 1758 |
| Berkåk | 1040 | 1260 | 1050 | 1350 | 910 | 1030 | 1107 |
| Oppdal | 1400 | 1820 | 1200 | 1650 | 1110 | 1280 | 1410 |
| T-O | 330 | 440 | 320 | 350 | 150 | 500 | 348 |
| O-B | 360 | 560 | 150 | 300 | 200 | 250 | 303 |

The lifting condensation level (LCL) at the three downhill stations, Oppdal, Berkåk and Tingvoll are listed in Table 4 for the storm situations given in Table 3, except for the missing observation at Berkåk, 10.03.82. Some interesting details are shown. First, Berkåk has the lowest, and Tingvoll the highest LCL. At Berkåk, LCL varies around 1000 m, which indicate

that the air has passed the lower mountains southeast of the station. The relative low LCL also at Oppdal show that the air is partly deflected around Rondane and Dovre, but has crossed some higher mountatins than Berkåk. The high value of LCL at Tingvoll shows that the air has crossed rather high mountatins southeast of the station. The air at Tingvoll therefore is very dry and warm.

Except from 31.01.95 (discussed in Chapt. 3), the non-damage storms have less difference of LCL between Oppdal and Tingvoll than the damage storms, where the LCL at Oppdal moves towards the values at Berkåk. This may indicate that the wind at a higher degree is deflected around Rondane and Dovre during the damage situations. For the approximately same wind speed, this indicate a more stable stratification. This is consistent with a picture of a stable layer of air near the crest, and lower stability higher up, giving a layer of trapped gravity waves in the atmosphere downstream the crest (see part II).

To get a further insight in the local winds at Oppdal, a full scale observational programme combined with numerical models should be made. The measurments should be carried out in the regions of damage risk, as well as upstream the local mountains Ålmanberget/Våtå-haugen. The models should cover the full mountain chain as well as the local mountains, for instance by a combination of the local model mentioned above and the larger scale numerical model discussed in part II. By doing this, both local forecasts and useful extreme wind information for building authorities could be given.

## 6. Summary and conclutions

5 damage wind storms at Oppdal during the periode 1994/95 has been discussed. Descriptions in local press for the last 20 years indicate that each of these storms has done more damage than any other storm in this period, and that this is due to the extremeness of the local wind.

Studies show that the critical wind sector of the wind aloft (1500 m level, above Oppdal) is 170 - 200°. The storms are found in situations where well-defined mesoscale mountain waves initiates energy transport down the lee-slope of the mountain chain. The model as well as the surface measurements show a warming of the air downstream, low wind speeds with a tendency to stagnation of the air upstream, and high wind speed at the downslope region.

Studies of LCL (lifting condensation level) derived from observations downstream indicate that the wind at a higher degree has been deflected around Rondane and Dovre during the damage situations. This is consistent with a picture of a stable layer of air near the crest, and lower stability higher up, giving a layer of trapped gravity waves in the atmosphere downstream the crest.

The storms seems to be connected to a horizontal vortex trailing out from Ålmanberget. The vortex is feeded from strong wind chanelling out the Ålmdalen valley and Våtåhaugen, probably strengthened by wind deflection around Rondane/Dovre.

The centre of the village have the largest risk of damage for wind aloft at 160 - 170°, while the risk area moves eastward when the wind direction turns south and southsouthwest.

The physics of the local wind response at Oppdal is not proved, but the theory is made reasonable. To get further evidence, or to come up with new theories, computer modelling where a small scale model covering the Ålmanberget area, and nested in larger scale meteorological models working at different scales, should be an interesting task to do. A full scale observation network covering Våtåhaugen and the risk area at Oppdal is needed for verification.

## 7. References

**Andresen, L. and Harstveit, K., 1993**
*Extreme wind analysis for Møre and Romsdal.*
DNMI/KLIMA report no. 07/93. In Norwegian.

**Eidsvik, K.J., Utnes, T., Sætran, L., Venås, B., Kubberud, N., and Nørstrud, H., 1994**
*Turbulent separated flows over hills.* ISBN No 82-7482-022-3,
NTH, Norwegian Institute for Technology, Trondheim, Norway.

**Jenkins, J., Mason, P.J, Moores, W.H., and Sykes, R.I., 1981**
*Measurements of the flow structure around Ailsa Craig, a steep, three dimentional, isolated hill.* Quarterly J. Roy. Met. Soc., 107, p.833-851, 1981.

# Part II

# Numerical simulations

List of content:

# 1. Introduction

Quite frequently several places in Norway are affected by strong windstorms. The present study is a part (Part II) of an investigation of five damaging windstorms in the small community Oppdal (62° 36' N, 09° 42' E) in Southern Norway in a one year period in 1994/1995.

Gravity waves forced by the mountains produce wind maxima along the lee slope of the mountains. These waves are identified in numerical simulations and verified in observational studies. Smith (1989) covers hydrostatic airflow over mountains. Several theories are proposed for the physical mechanism producing the wind maxima in the cases with particular strong winds. A review and discussion of those is given by Durran (1990).The phenomenon is often referred to as downslope windstorms and are known to occur along mountain barriers throughout the world. Downslope windstorms forced by the Rocky Mountains and affecting Boulder, Colorado might be the most well-known. Numerous papers handles "Boulder cases". Several places in Norway are also affected by the phenomenon although the documentation is scarce.Mesoscale measurements of windstorms by Doppler lidar measurements in the Boulder area are presented in Neiman et al. (1988). In Norway only conventional observations are available and the observational documentation may be sparse.

There are several reasons for studying the conditions for downslope windstorms in Norway. There is a need for understanding downslope windstorms and for establishing rules or guidance for operational forecasting of such events. Severe damage on buildings and other constructions have been reported. For construction purposes both frequency and maximum winds are needed locally. The Norwegian mountains are rather complex and three dimensional simulations are needed to describe the flow. The position in the westerlies with sea areas upstream makes, however, the frontal analyses relatively simple at least before the fronts reaches the mountains. Our three dimensional simulations of Norwegian windstorm cases should hopefully contribute to the understanding of the conditions for the downslope windstorm phenomenon. In addition, the study is also motivated by the interest in how the model can handle the flow over the mountains in Norway. For this purpose, those five strong wind cases are quite interesting.

In the present study we will document the five cases as observed and simulated with the operational numerical weather prediction model at DNMI. The model is hydrostatic and the horizontal grid has a 50 km resolution. We must emphasize that the local winds in the complex terrain in the Oppdal area can not be simulated in a model simulation with 50 km grid.The aim of the study is to look into the model simulations in order to test the relevance of the model simulations on the scale they can resolve. Investigation of the topography in Oppdal and suggestions for the effects responsible for the damage are presented in Part 1. One of the five cases has also been simulated in a nested higher resolution run (10 km grid). The topography in Southern Norway is however so complex that even this is far too smooth as compared to the local topography.

In the next section we discuss and present the numerical models. The third section deals with the simulations. In the forth section, we discuss common features of the storms and their simulation.

There are plans at the Norwegian Meteorological Institute (DNMI) for using the five present cases for testing higher resolution models and non hydrostatic models. There is also plans for applying local wind models with a resolution of hundred meters in the local area around Oppdal

and for extending the measurements program in the Oppdal area. Eventually more observations will then be available for studying Oppdal windstorms in the future.

## 2. The numerical models.

The operational mesoscale model (LAM50S) at DNMI is used for this study (LAM50S was replaced by a version of the HIRLAM model 13.6.95) The documentation of the adiabatic formulation in the prediction model in LAM50S is given by Grønås and Hellevik (1982). The parameterization of physical processes is described by Nordeng (1986). The model is based on the primitive equations (using the hydrostatic assumption in the vertical). The vertical sigma-coordinate is scaled by the surface pressure so the horizontal grid follows the model surface. The data assimilation in the operational use is based on a method from Bratseth (1986). The implementation of the data assimilation is described by Grønås and Midtbø (1987). LAM50S is operated on a polarstereographic horizontal grid with 50 km resolution at 60 N. There are 31 levels in the vertical. The data assimilation cycle is six hours.

The model resolution of 50 km is far too coarse to describe the detailed Norwegian mountains. The model mountains are accordingly a marked smoothing of the real topography. Details in the stratified flow over and/or around mountains on a horizontal scale above about 200 km (4 times the grid separation) can be described by the LAM50S model resolution. This means that the largest scale of the Scandinavian mountains are resolved. The effect of smaller scale details in the topography on the flow can of course not be described. A hydrostatic model with parameterization of vertical diffusion will avoid static instability. A phenomenon like wave breaking which include static instability mechanisms can not be adequately described in such a model. The way the model controls static instability will be discussed in the last section

Data from LAM50S has been used for this model based study of the five cases. The area of integration (Figure 1) has been reduced as compared to the operational area. As lateral boundary data we have used analysis from ECMWF while the operational model uses prognosis. The model has been integrated for more than six hours without introducing observations. Several start times for the integration has been tried in order to find the best simulations. The integrations time used is from +15 up to +30 hours. Below the five cases will be presented and discussed as simulated by the 50 km model. Date and some information about the cases are included in table 1.

A version of LAM50S with a 10 km grid (LAM10) has been nested inside the 50 km run.The number of vertical levels are the same. The area of LAM10 is also shown in Figure 1. The 10 km model topography is shown in figure 12.

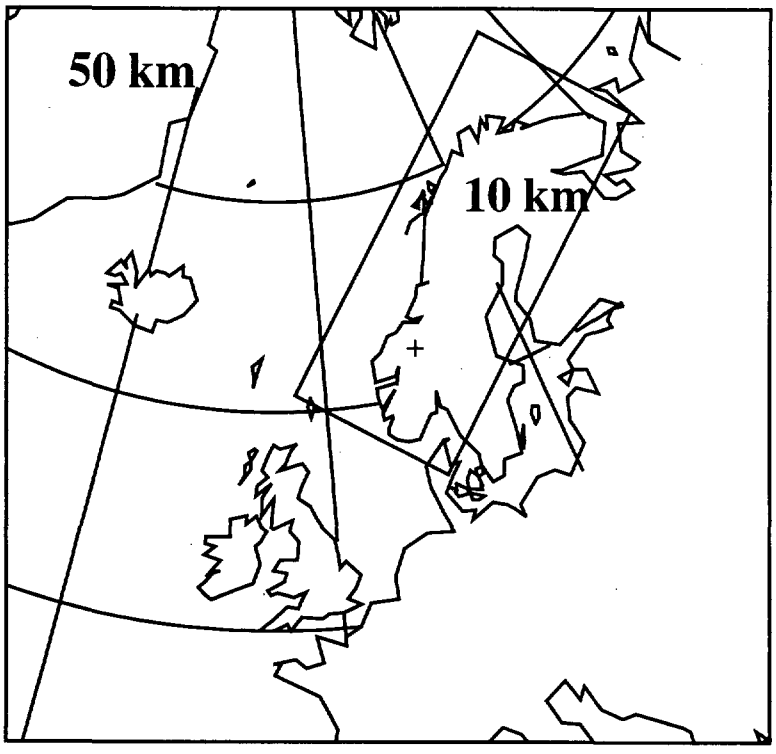


Figure 1. Area of integration for LAM50S used in this study. Area for the nested 10 km model is the small area. Position of Oppdal is marked with a cross.

## 3. Simulation of 5 windstorms at Oppdal in Southern Norway

### 3.1 Simulations of five cases with LAM50S.

The LAM50S topography is so that the along flow scale is similar to the cross-flow scale as can be seen in figure 2. We will in the following present model level data and two dimensional cross-sections remembering that the simulated data has a complicated three dimensional structure. The largest horizontal scale of the mountains is so that the coriolis effect has to taken into account for the flow across the mountains (for L= 500km and U =20 m/s, the Rossby number is about 1/4).

The height of Oppdal in the 50 km topography is 1280 m. while the observation site in the Oppdal valley is situated 668 m above sea level.

The cases are referred to by letters from a-e. The date and approximate time of the strongest winds in the LAM50S simulations are given in the table above.

Positions of all cross-sections displayed here are given in Figure 3. The frontal structure has been studied by the use of conventional observations, horizontal maps and cross-sections from the model simulations. Synoptic surface maps valid at the time of the strongest wind in the simulation (or a few hours ahead) have been prepared and are shown in Figure 4.a-e. For case

a and b the maps are for the times in the table above while for case c-e the maps are valid 3 hours earlier.The most difficult part of the surface analysis is the positioning of the fronts close to the mountains as the fronts are modified by mountain effects. SYNOP wind reports are included in figure 5a-e for the UTC times given in table 1. The observations are included for information. Local winds in Oppdal are covered by Part I where maps of the local area, the observation sites and the damage areas are included. The observation is subjective as there is no anemometer at the station. Estimation problems might therfore reduce the accuracy of the observations. We must stress that even if it is an observing site in the Oppdal community, it is not representative for the damaging wind locally. A complicating factor for the evaluation of the simulations, is that we have no representative anemograms from the area to identify the accurate time of the windstorm.

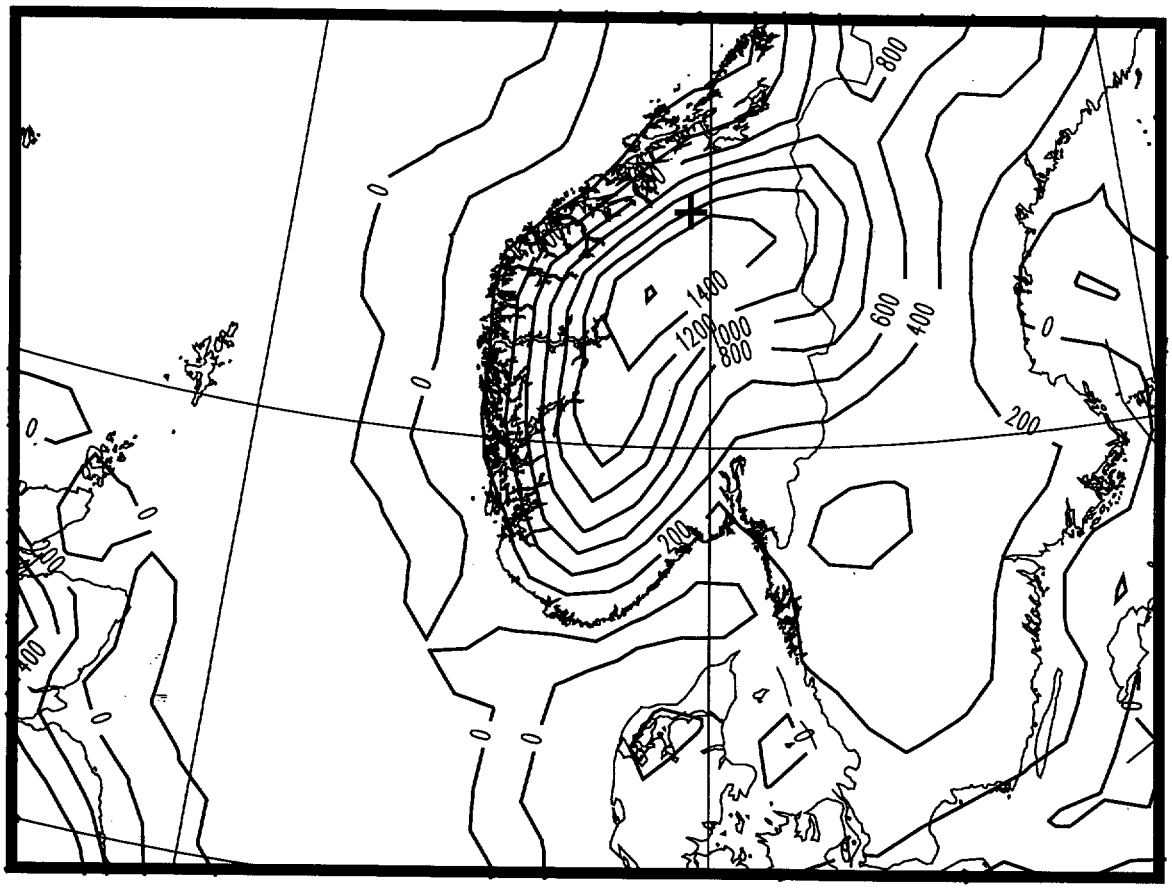


Figure 2. Part of the topography used in the LAM50S model. Isolines for every 200 m. The position of Oppdal is marked by a cross

The cross-sections used around the time of the strongest wind is Aa and Bb trough Oppdal from south to north (Figure 6 a-e) and from west to east (Figure 7.a-e) respectively. Maps of simulated wind in model level 27 are given in Figure 8a-e. Model soundings and available TEMPs from the stations Ørlandet and Gardermoen are given in Figure 9a-d and 10a-d. Positions of Gardermoen and Ørlandet are given in Figure 3. In Figure 11 we have included copies of pressure readings (barograms) from the observing site in Oppdal.

**Table 1:**

| CASE | DATE | TIME | ff max. | ff fixed | surface map valid at | SYNOP map valid at |
|---|---|---|---|---|---|---|
| a | 31.03.94 | 09 UTC | 39 m/s | 28 m/s | 09 UTC | 12 UTC |
| b | 08.12.94 | 18 UTC | 47 m/s | 33 m/s | 18 UTC | 18 UTC |
| c | 18.01.95 | 09 UTC | 52 m/s | 37 m/s | 06 UTC | 12 UTC |
| d | 20.01.95 | 09 UTC | 45 m/s | 35 m/s | 06 UTC | 12 UTC |
| e | 31.01.95 | 15 UTC | 51 m/s | 42 m/s | 12 UTC | 18 UTC |

Table 1. Date and approximate time for the strongest simulated wind in the Oppdal area. The maximum simulated wind above Oppdal is given in the ff max. column.The value of the wind at a fixed height (1700 m above sea level) above Oppdal is given in the next column (ff fixed). Time in UTC for the surface maps in Figure 4a-e and SYNOP maps in Figure 5a-e are given in the two last columns. The height of 50 km topography at Oppdal is 1280 m.

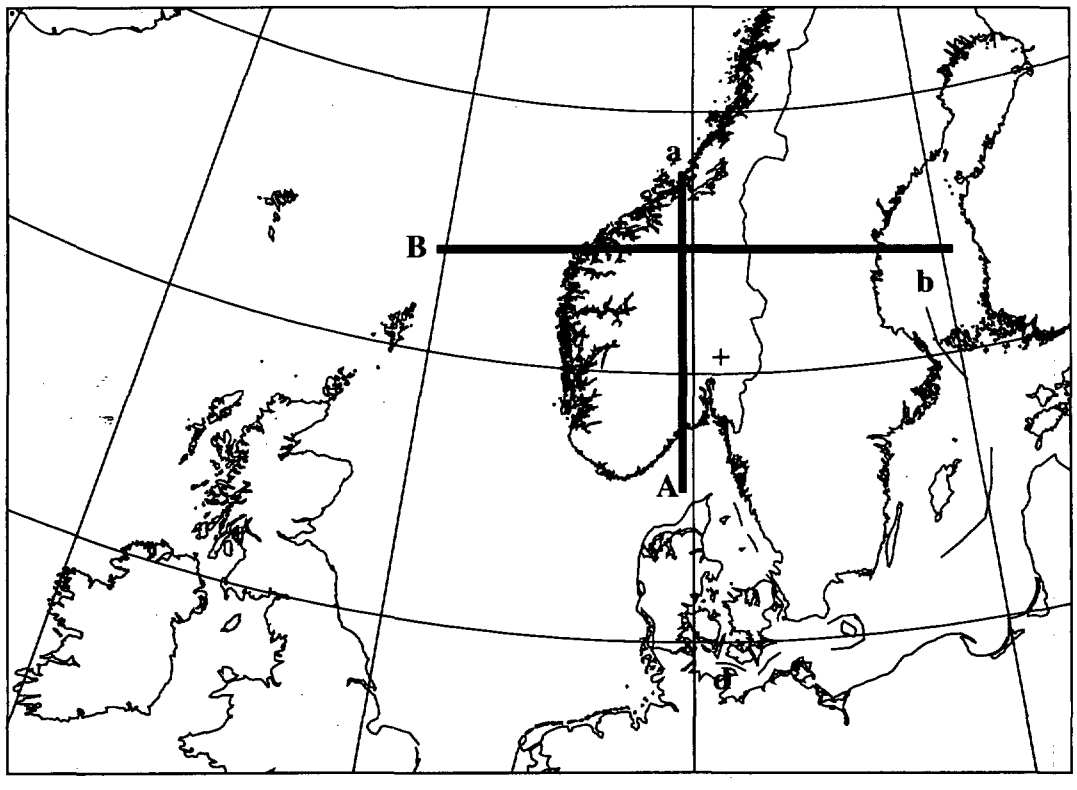


Figure 3. Position of the two different cross-sections displayed in this report. The sections are referred to as Aa and Bb.The Capital letter is to the left in the cross-section Figures 4 a-e and 5 a-e. The observation site Gardermoen is marked by a cross east of cross-section Aa. Ørlandet is at the northern end of cross-section Aa.

### 3.1.1. Case a 31.03.94

Surface map valid 09 UTC 31.03.94 is shown in Figure 4a. A deep low (948 hPa) is found north of Scotland. An occluding frontal wave has reached Southern Norway from SW. The warm front of the occlusion is about to pass the Oppdal area. The surface report from Oppdal (Figure5a) is reporting a past wind force maximum of 64 knots.

Inspection of cross-sections at 06 UTC south of Norway (not shown), showed a southerly low level wind maximum of above 20 m/s ahead of the warm front. Increased static stability at lower levels was connected to the front.

The cross-sections trough Oppdal in Figures 6a and 7a are valid 09 UTC. The cross-section from south to north (Figure 6a) shows tilting mountain waves with a wind maximum of 39 m/s at 1500 m height above sea level (above Oppdal). Upstream of the mountains the static stability has a maximum between 700 and 850 hPa. The possibility of reflection connected to this maximum will be discussed in section 4.

The simulated warm front (Figure 7a) is now sloping along the western side of the model mountains. Wind at model level 27 (third arrows from bottom in Figure 6a) is shown in Figure 8a. The wind has reached a maximum of above 40 m/s to the west of the top of mountains.

The TEMPs at 12 UTC can be compared to the simulated ones in Figures 9 a and.10 a. The low level wind maximum at Ørlandet on the lee side (65 kts at 850 hPa) is well simulated. The simulated inversion layer below 850hPa is however somewhat exaggerated at a too low elevation. At Gardermoen, the wind at lower levels is too high in the simulations. Also here the inversion is exaggerated and placed too low. This might be connected to improper simulation of static instability and will be discussed in section 4.Despite of these errors, the model seems to have captured the synoptic scale features quite well. The wind variation around and over the Norwegian mountains is also in reasonable agreement with observed vertical structures at the two soundings at Ørlandet and Gardermoen.

The barogram in Figure 11 has secondary minimum at 11 UTC which is probably the mesoscale pressure drop as the front passes Oppdal.

### 3.1.2. Case b 08.12.94

The surface map in Figure 4b is valid 18 UTC. A deep low of 962 hPa is situated just outside Southern Norway. A warm occlusion is about to pass Oppdal. Oppdal reports 25 knots.

When the frontal system passed England about 06 UTC, the low-level wind maximum ahead of the warm front was simulated to 33 m/s. Connected to the front is an increased stability of the lowest layers.

The cross-sections through Oppdal are valid 18 UTC (Figures 6b and 7b).In the south to north cross-section we see that the static stability is much lower than in case a. A slightly more stable layer is seen above mountain top level. Over this layer there is a third less stable layer. The wind has a maximum of 47 m/s at about 1800 m height. Comparing to case a, there is a difference in the wind shear. There is now a strong increase and veering of the wind throughout the troposphere. The Richardson number is low as a result of the shear and the critical layer effect can therefore be active. Discussion will again be done in section 4.

a

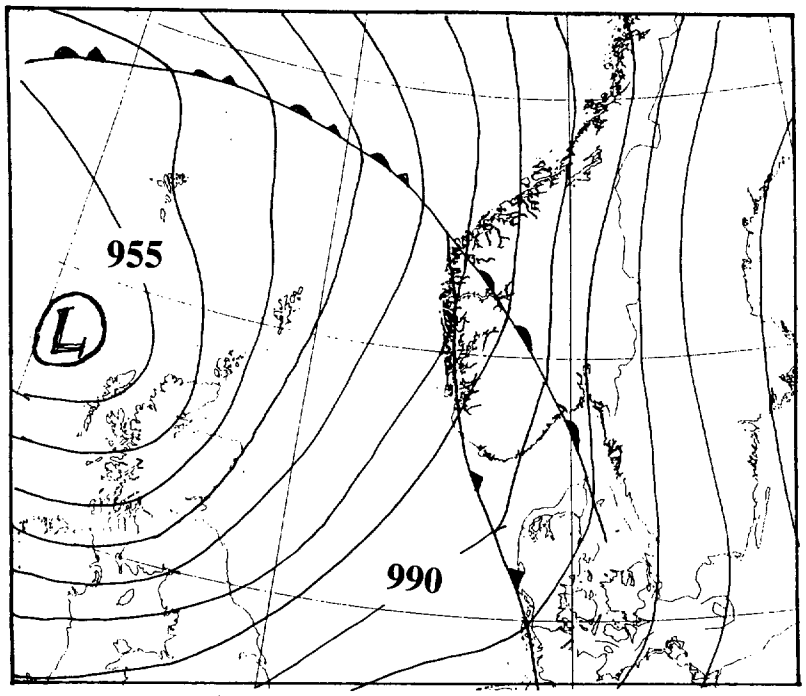


b

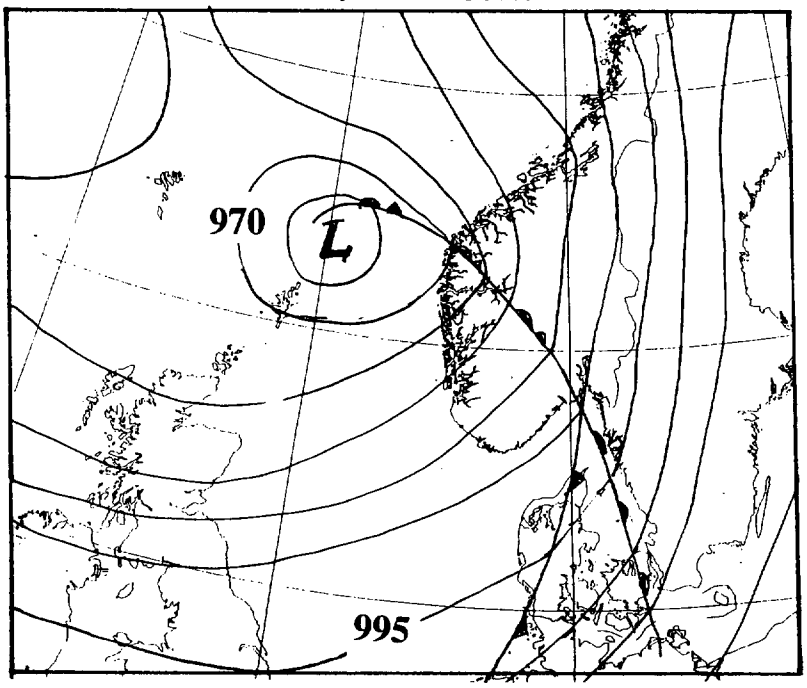


c

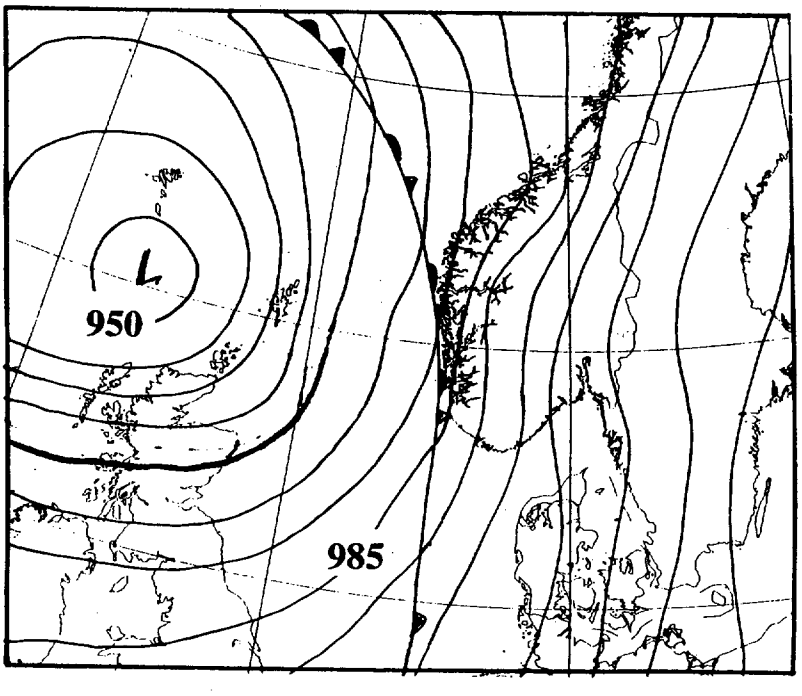

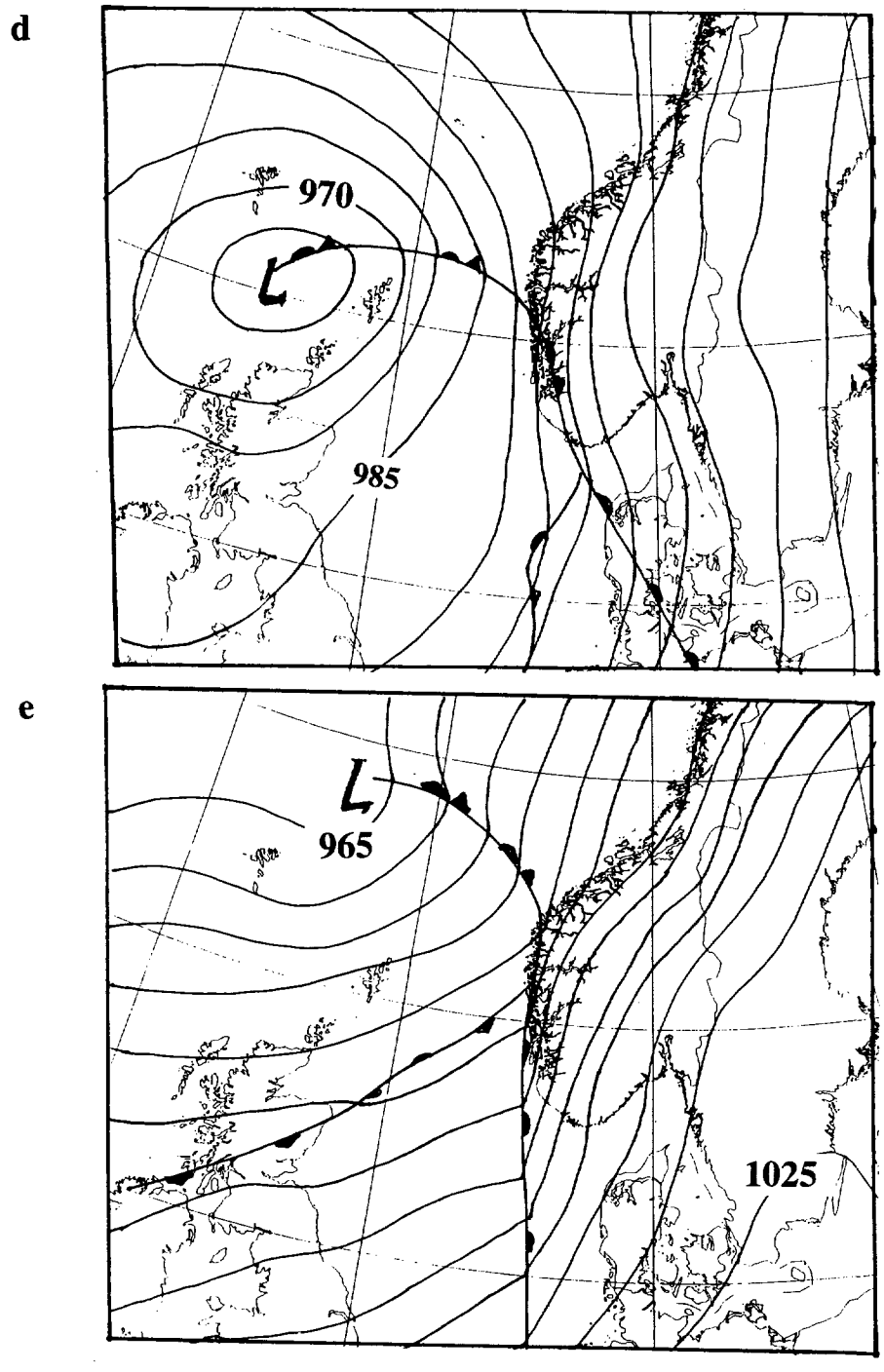


Figure 4 a-e. Surface analysis for the five cases a-e. Pressure labels in hPa.
Case a: Valid 09 UTC 31.03.94
Case b: Valid 18 UTC 08.12.94
Case c: Valid 06 UTC 18.01.95
Case d: Valid 06 UTC 20.01.95
Case e: Valid 12 UTC 31.01.95

a

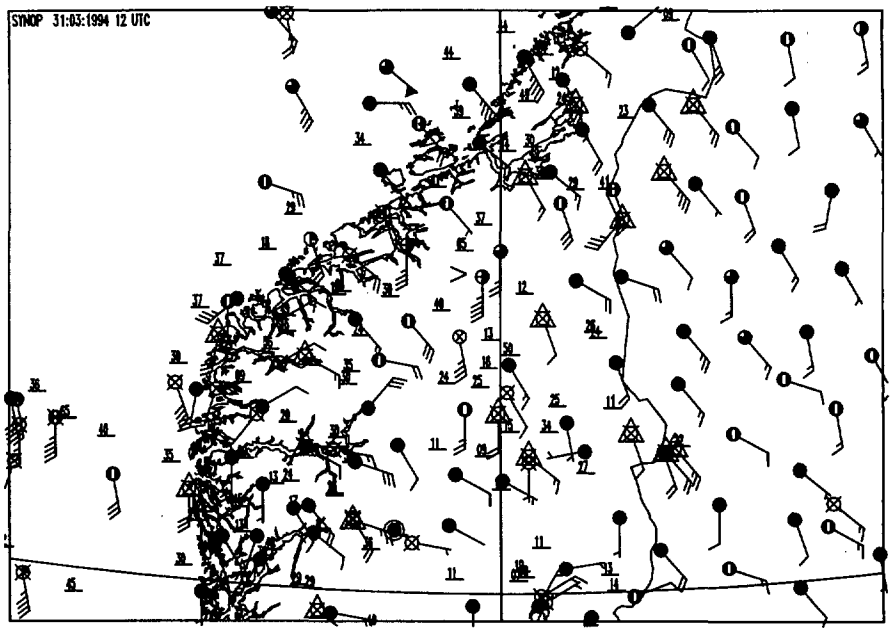
SYNOP 31:03:1994 12 UTC

b

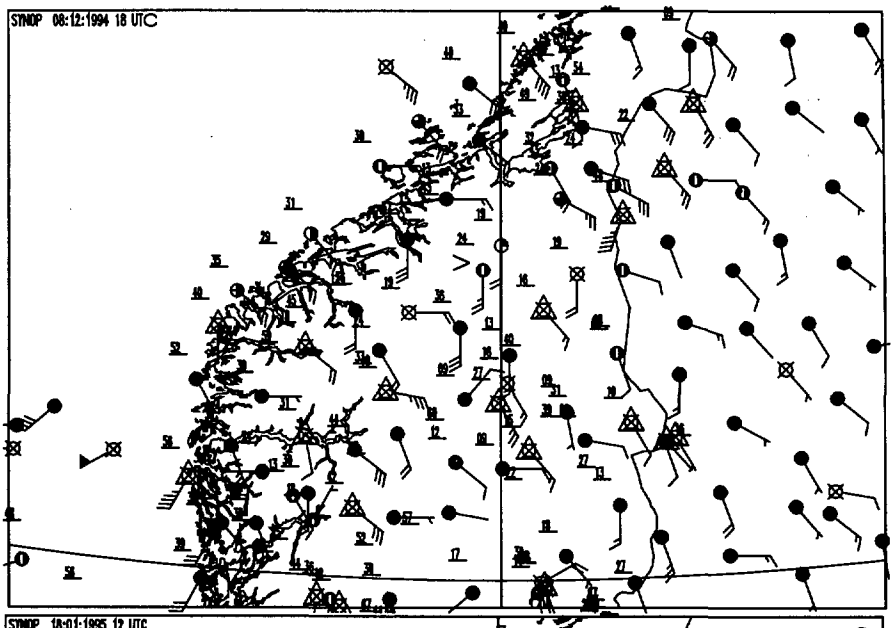
SYNOP 08:12:1994 18 UTC

c

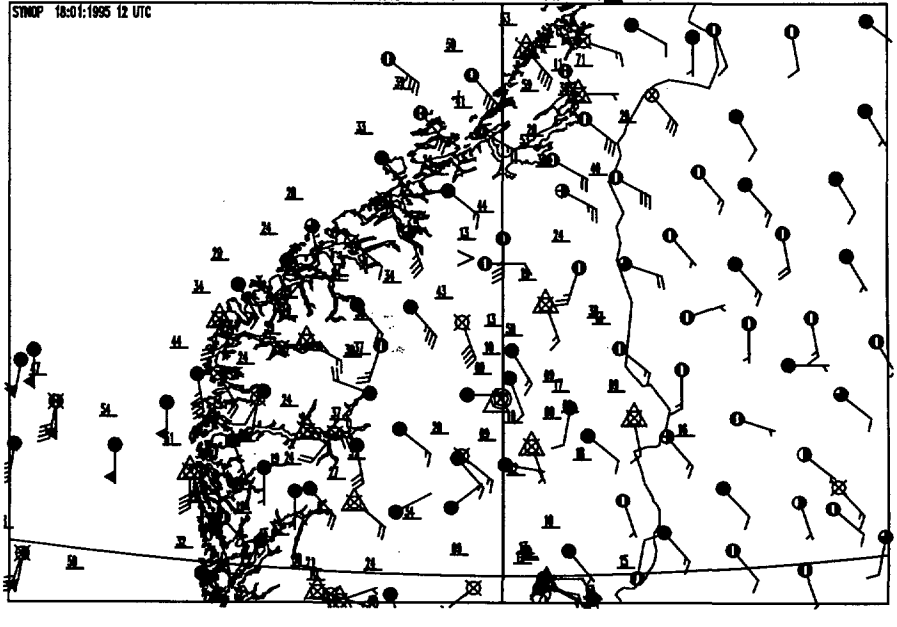
SYNOP 18:01:1995 12 UTC

d

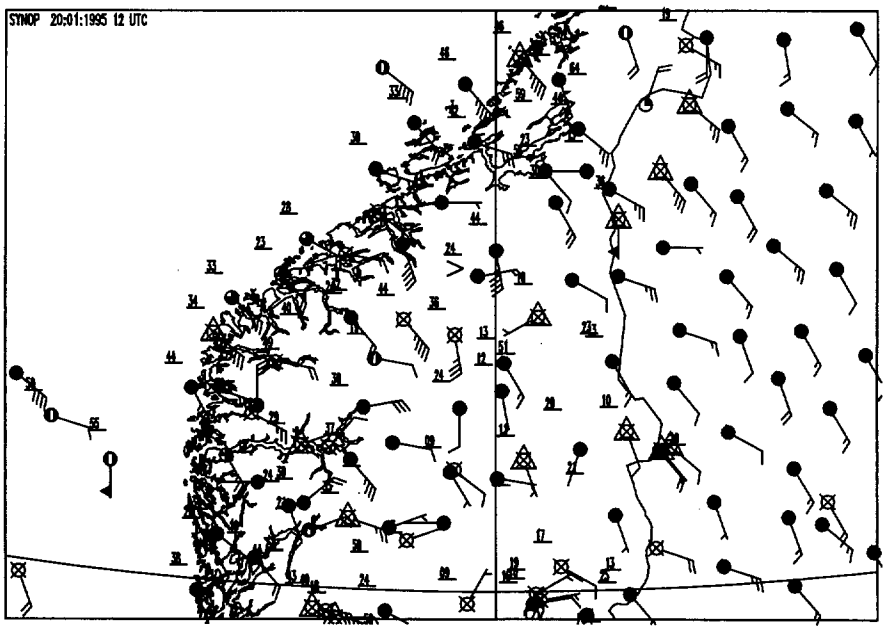


e

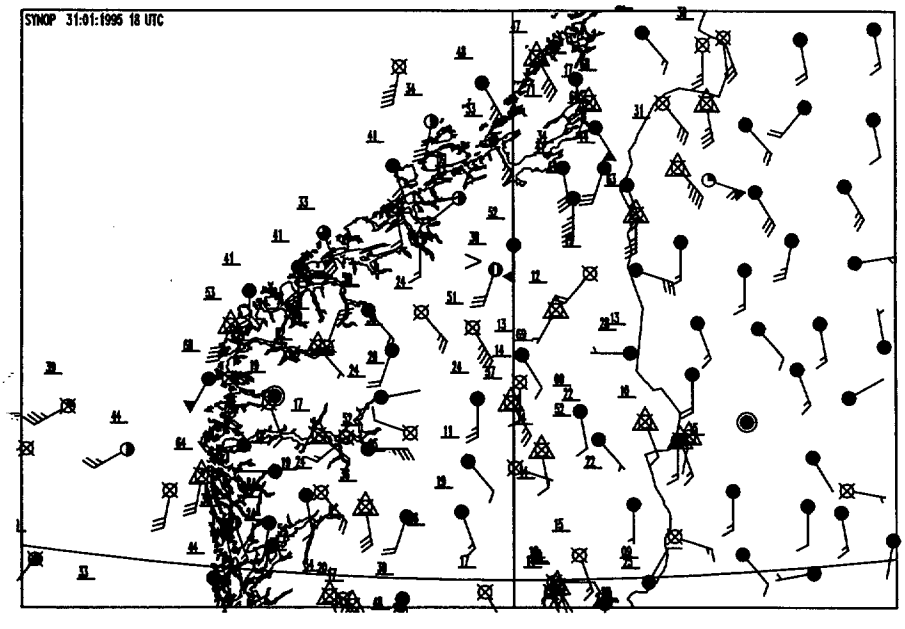


Figure 5a-e. Observed winds (arrows giving knots) and maximum wind force since last observation (knots, underlined number upper left for station. Non-automatic stations are marked by a circle filled according to octas of clouds (crossed circle means octas not given). Automatic stations are marked by a triangle. > points at Oppdal from left.
Case a: Observations at 12 UTC 31.03.94
Case b: Observations at 18 UTC 08.12.94
Case c: Observations at 12 UTC 18.01.95
Case d: Observations at 12 UTC 20.01.95
Case e: Observations at 18 UTC 31.01.95

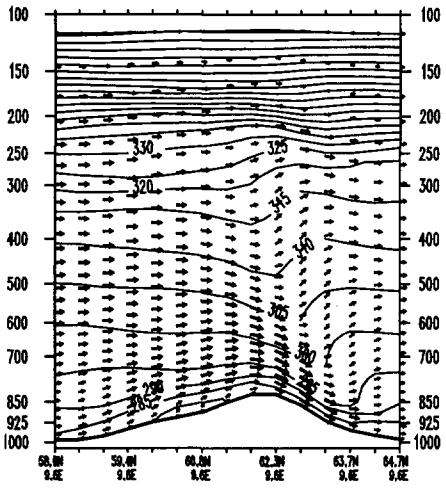


a

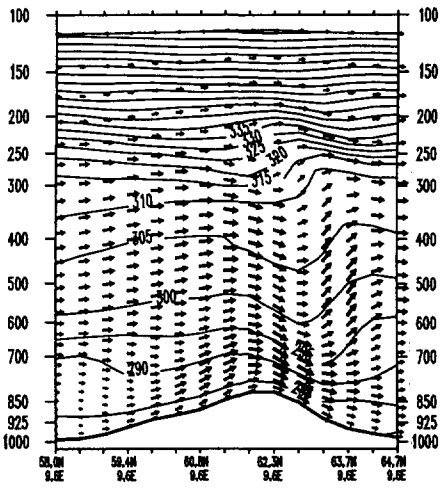


b

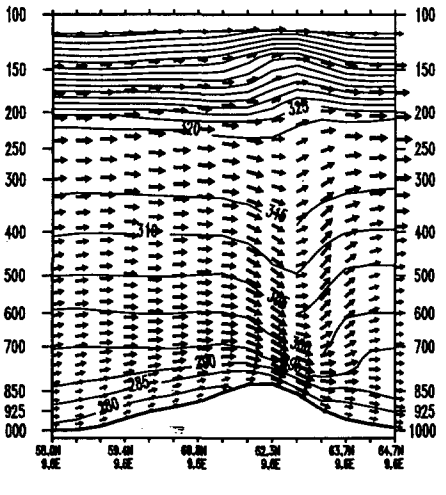


c

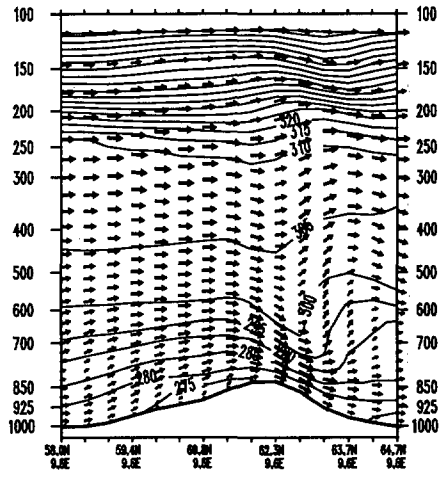


d

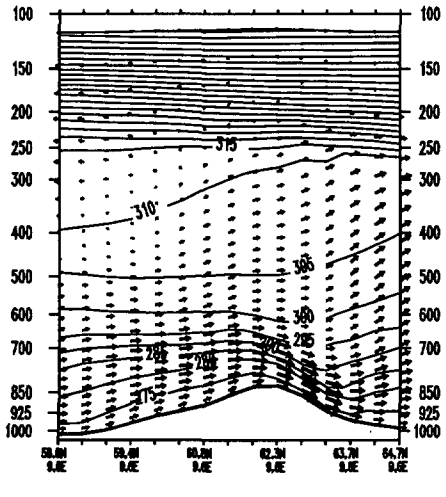


e

Figure 6 a-e. LAM50S cross-section Aa for the cases a-e (from top left).
Vertical axis is pressure (hPa).
Positions in degrees along the horizontal axis (decimal).
Solid lines give potential temperature.
Arrows give tangential displacement in 12 minutes.
Decimal position of Oppdal is62.60 N and 09.70 E

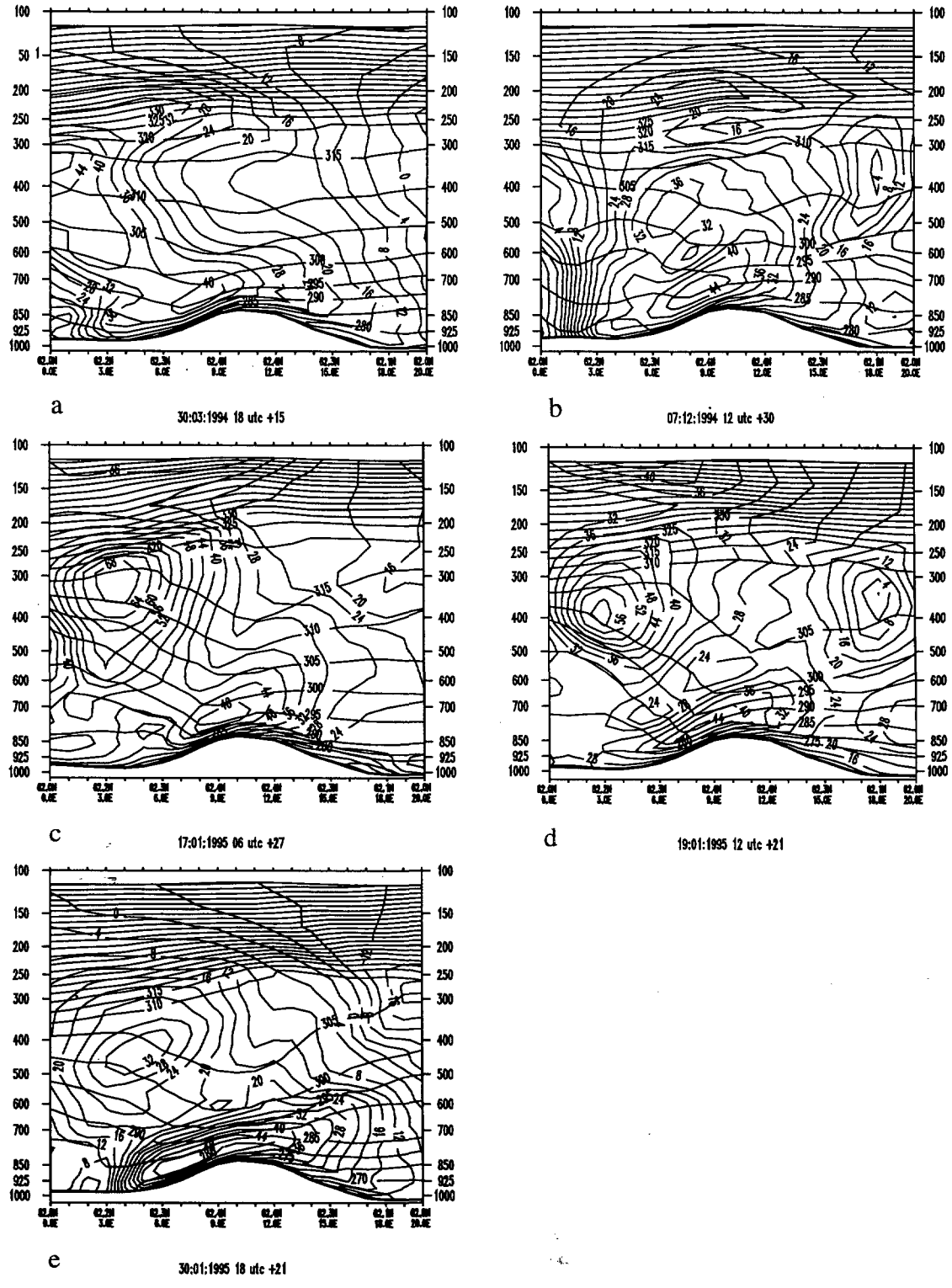


Figure 7 a-e. LAM50S cross-sections Bb for the cases a-e (from top left). Vertical axis is pressure (hPa). Positions in degrees (decimal) along the horizontal axis. Solid lines give potential temperature (K) and wind component normal to the plane (m/s).Decimal position of Oppdal is 62.60 N and 09.70E.

a

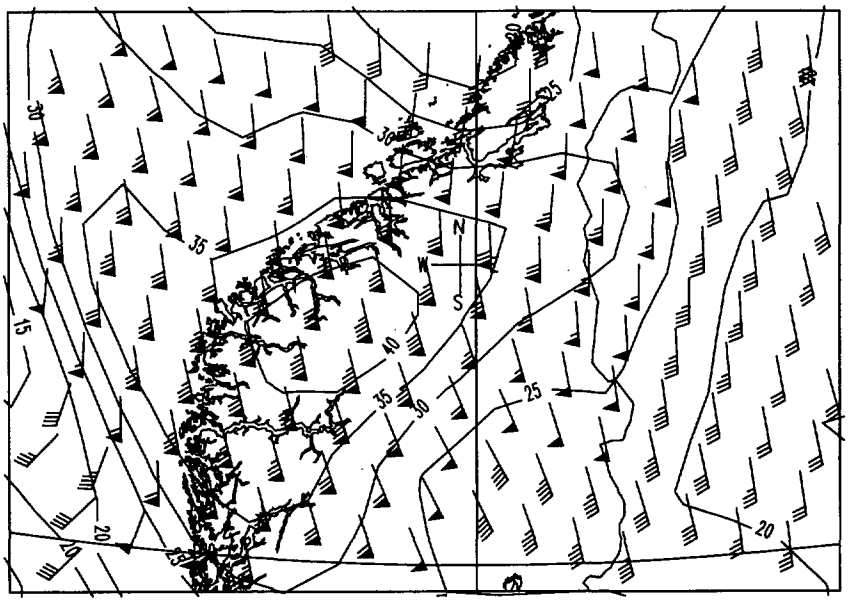

b

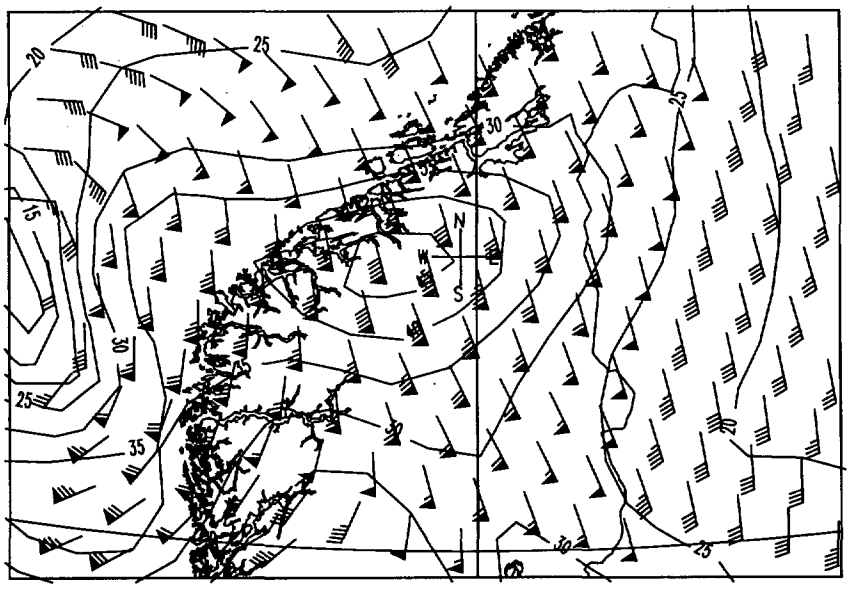

c

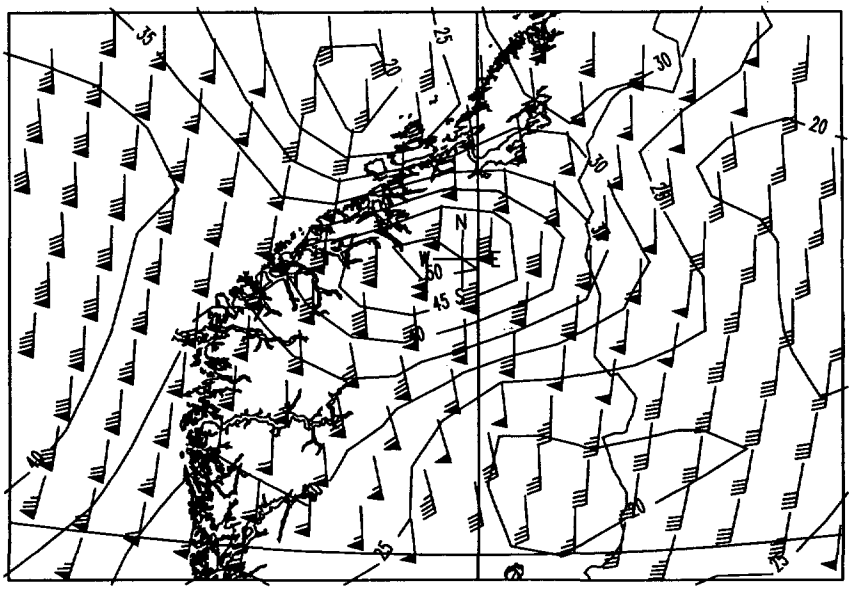

d

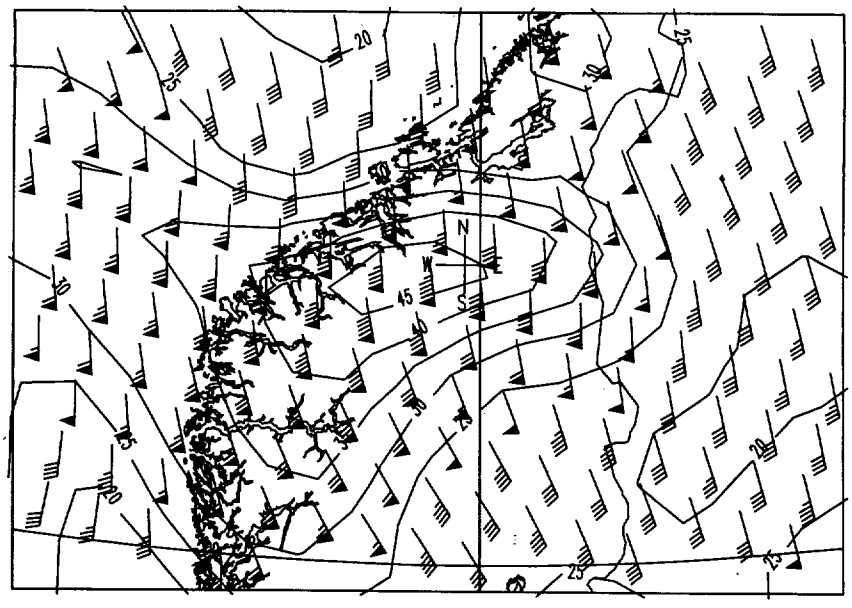

e

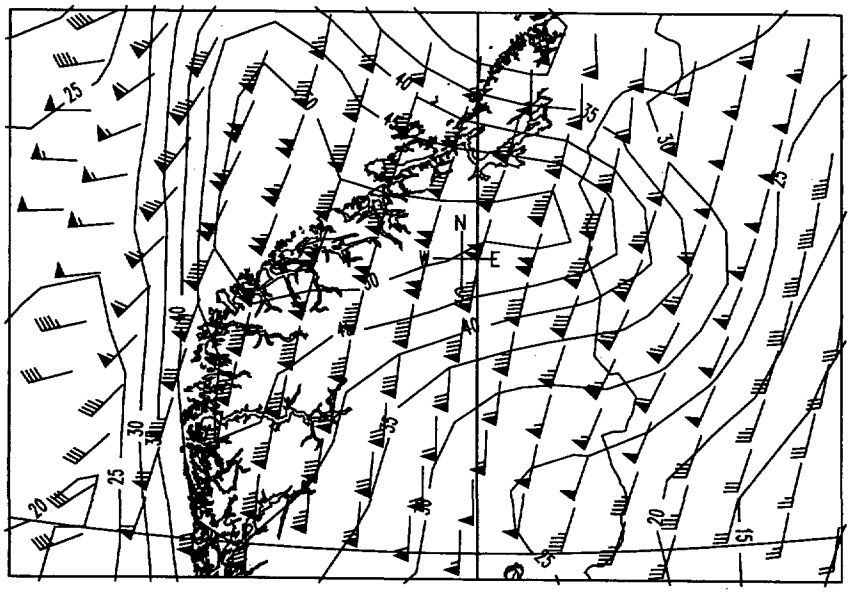

Figure 8 a-e. Maps of simulated wind in LAM50 model level 27 for the five cases a-e (third arrows from the bottom in the cross-sections in Figures 6 and 7 is for the same level). Wind arrows (knots) and isolines of wind speed (m/s). A cross (with direction letters S,E,N,W) marks the position of Oppdal

Case a: Valid 09 UTC 31.03.94 (+15 hours integration)
Case b: Valid 18 UTC 08.12.94 (+30 hours integration)
Case c: Valid 09 UTC 18.01.95 (+27 hours integration)
Case d: Valid 09 UTC 20.01.95 (+21 hours integration)
Case e: Valid 12 UTC 31.01.95 (+21 hours integration)

a

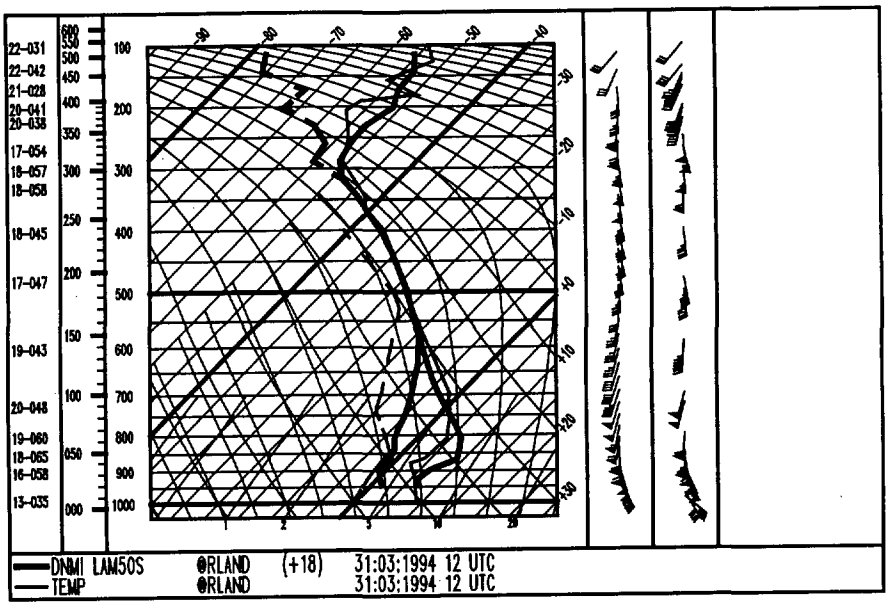
DNMI LAM50S @RLAND (+18) 31:03:1994 12 UTC
TEMP @RLAND 31:03:1994 12 UTC

b

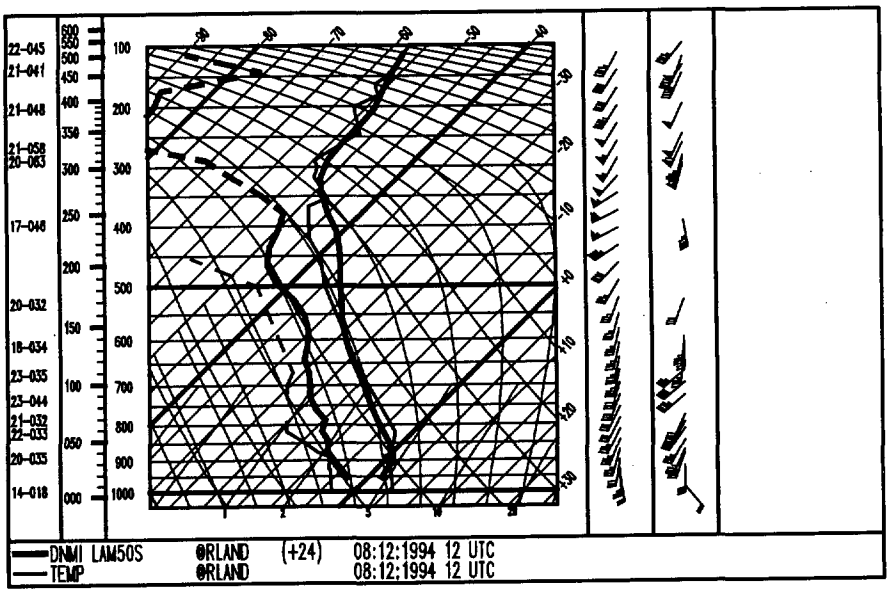
DNMI LAM50S @RLAND (+24) 08:12:1994 12 UTC
TEMP @RLAND 08:12:1994 12 UTC

c

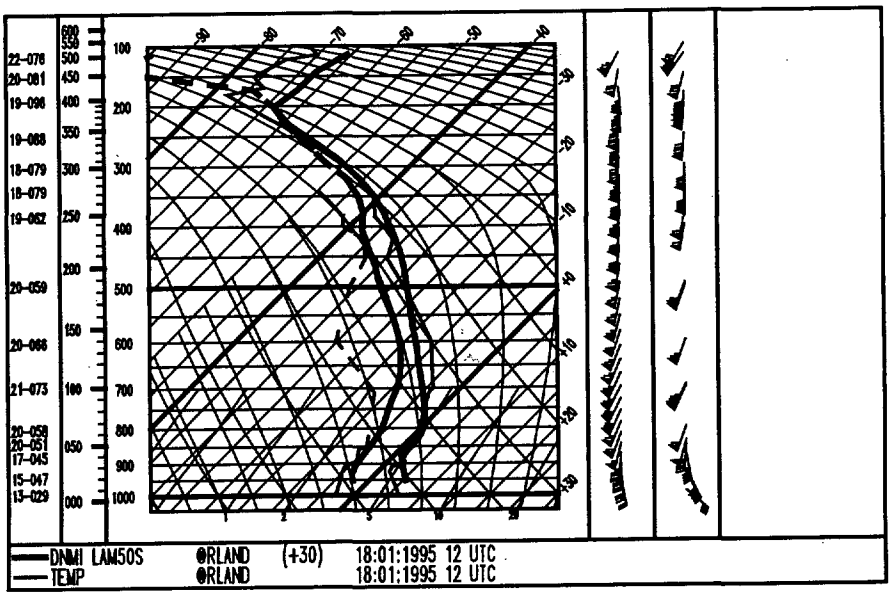
DNMI LAM50S @RLAND (+30) 18:01:1995 12 UTC
TEMP @RLAND 18:01:1995 12 UTC

d

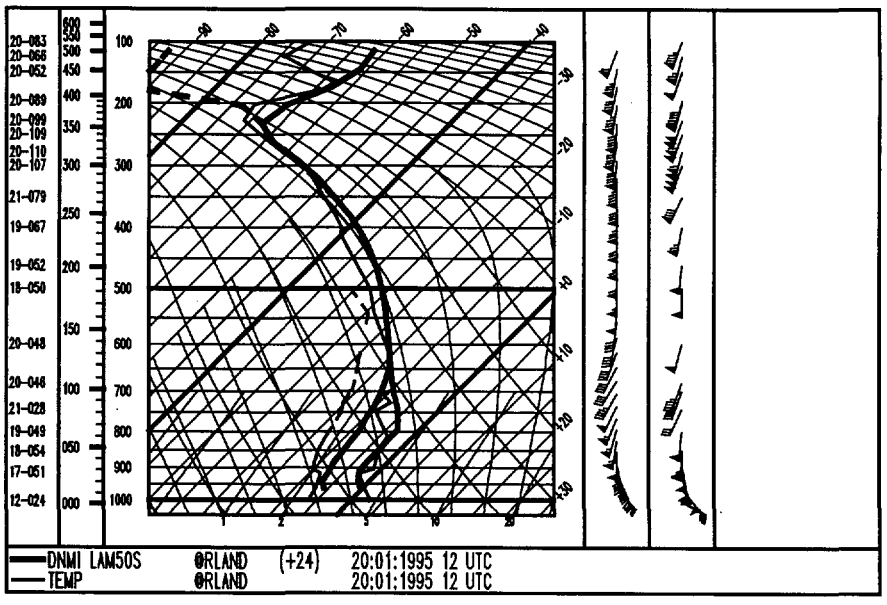


e

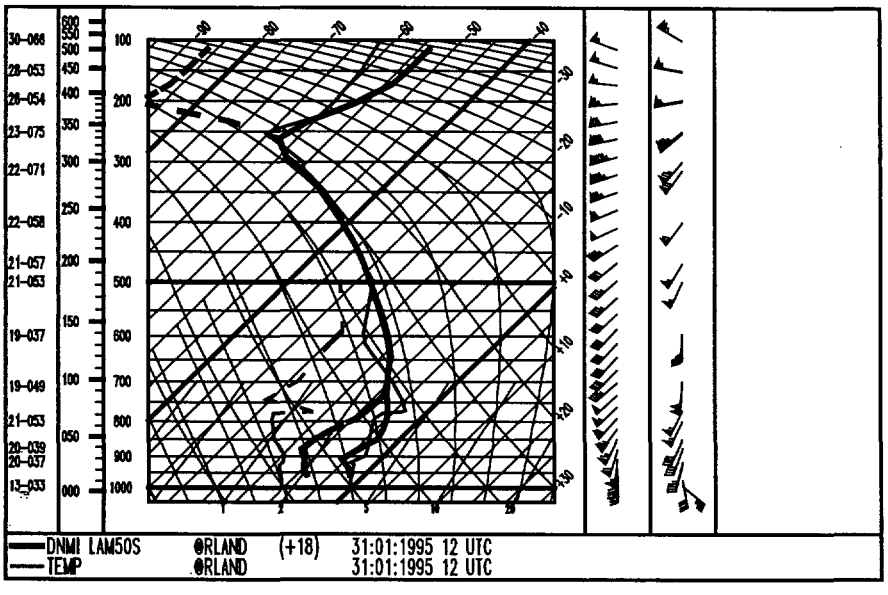


Figure 9 a-e. Simulated LAM50S vertical profiles (thick lines) and observed vertical profiles (thin lines) of temperature and dew point at Ørlandet. The diagram is an Amble diagram which is a skew T, ln p diagram below 500 hPa and a skew T, p diagram above. Wind arrows for the simulated 30 levels and observations are given in two columns to the right in the Figure. Some wind observations are for technical reasons plotted on top of each other. Selected observed winds are, however found as direction (tenths of degrees) and force (knots) in the left part of the figure.

a

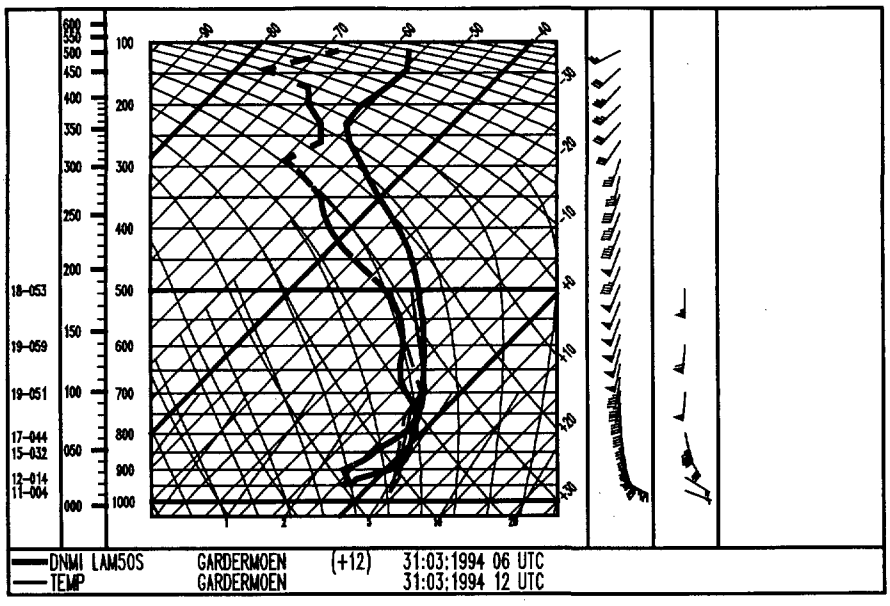
DNMI LAM50S GARDERMOEN (+12) 31:03:1994 06 UTC
TEMP GARDERMOEN 31:03:1994 12 UTC

b

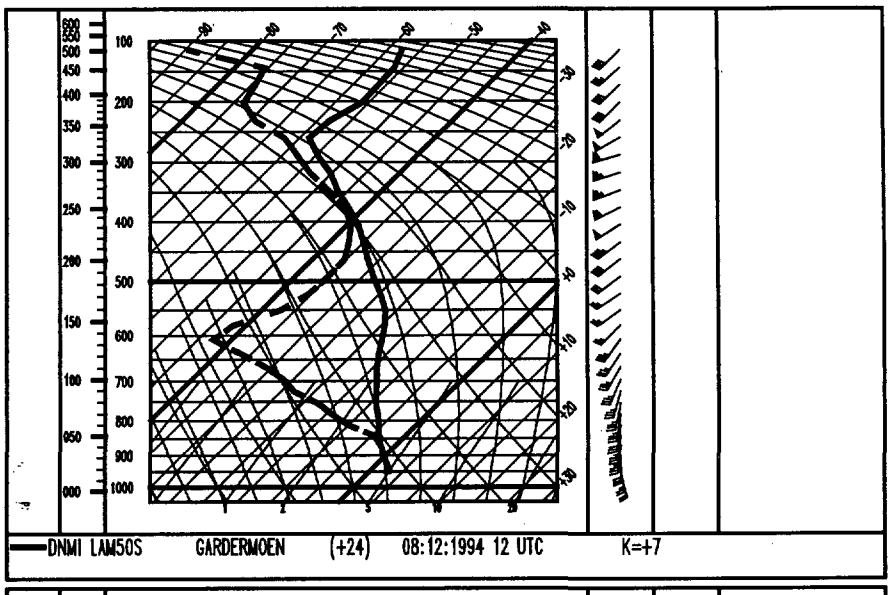
DNMI LAM50S GARDERMOEN (+24) 08:12:1994 12 UTC K=+7

c

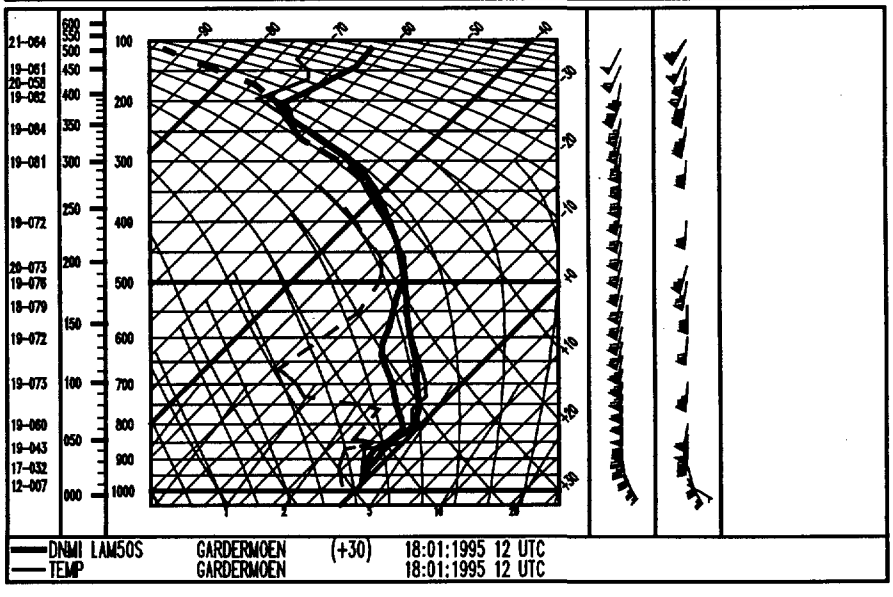
DNMI LAM50S GARDERMOEN (+30) 18:01:1995 12 UTC
TEMP GARDERMOEN 18:01:1995 12 UTC

d

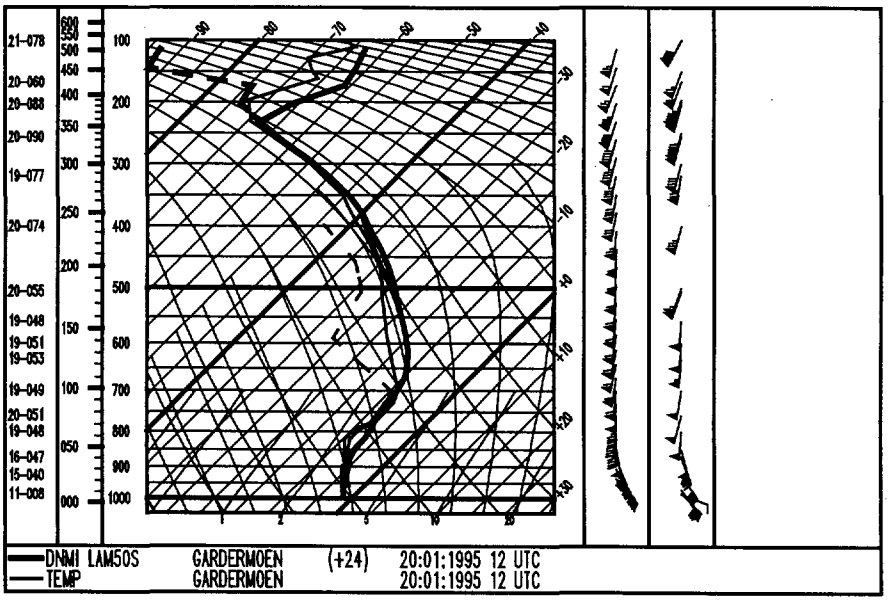


e

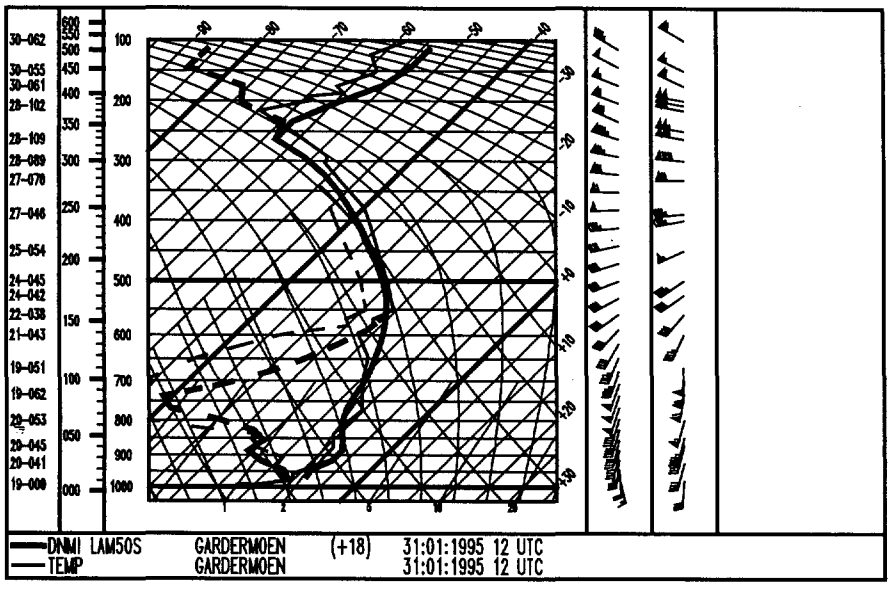


Figure 10 a-e. Simulated LAM50S vertical profiles (thick lines)and observed vertical profiles(thin lines) of temperature and dew point at Gardermoen. The diagram is an Amble diagram which is a skew T, ln p diagram below 500 hPa and a skew T, p diagram above. Wind arrows for the simulated 30 levels and observations are given in two columns to the right in the figure. Some wind observations are for technical reasons plotted on top of each other. Selected observed winds are, however found as direction (tenths of degrees) and force (knots) in the left part of the figure.

The cross-section from east to west shows the sloping weak warm front. The occlusion is sloping along the western side of the mountain. Wind in model level 27 is shown in Figure 8b. The simulated wind maximum of 47m/s is again to the west of the mountain top. The gravity waves are seen troughout the troposhere.

TEMP observation at 12 UTC from Ørlandet (Figure 10.b) shows in this case structures in the wind profile which are present in the model data. As a hypothesis we suggest that this is due to lack of model resolution.

The barogram shows some rapid fluctuations in the pressure (order of minutes). The minimum at 21 UTC is connected to the frontal passage.

### 3.1.3. Case c 18.01.95

The surface map valid 06 UTC in Figure 4c shows a very deep low of 948 hPa north of Scotland. In this case an occluded front is crossing southern Norway from WSW. The station at Oppdal reported 12 UTC a past maximum wind force of 13 knots (Figure 5c).

Generally strong winds of about 40m/s were simulated ahead of the front as it approached Norway. The increased stability connected to the warmer side of the occlusion was modest compared to the other cases.

The cross-sections valid at 09 UTC are shown in Figures 6c and 7c. A tilting mountain wave throughout the whole troposphere is seen in Figure 6c. The wind maximum is now 52 m/s at about 2000 m height above Oppdal. The stability near the mountain top si increased, however, less than in the other cases. Since the amplitude of the mountain waves in this case is maintained throughout the tropopause, we will suggest some reflection in this case is caused by the tropopause. We return to this in section 4.

Winds at model level 27 in Figure 8c and the cross-sections also show a wind maximum to the west of the mountain top of more than 50 m/s. The occluded front is also seen in Figure 7c.

We find agreement between simulated and observed (TEMP) wind at both Ørlandet and Gardermoen (Figures 9c and 10c). The temperature profile is also broadly correct.

The barogram shows again small scale fluctuations. The minimum at 09 UTC is connected to the frontal passage.

### 3.1.4 Case d 20.01.95

Surface map valid 06 UTC is given in Figure 4d. A low of 963 hPa is found north of Scotland. An occlusion followed by a secondary wave on the cold front passes Southern Norway from SSW. The report from Oppdal at 12 UTC (Figure 5d) gives a past maximum of 24 knots.

Connected to the warm front increased low-level stability can be seen in both cross-sections trough Oppdal valid at 09 UTC (Figures 6d and 7d). There is a stability maximum above mountain top upstream (top at about 700 hPa). The gravity wave has a reduced amplitude above this level. The wind maximum above Oppdal is now 45 m/s at about 1600 m height.

The cross-section 7d and the model level 27 winds shows a wind maximum of a little above 45 m/s northwestwards of the mountain top.

The Temp observations show discrepancies at Gardermoen as the model gives a smoother temperature profile. Downstream at Orlandet there are again details in the temperature profile not simulated by the model. The simulated wind variations are, however, in better agreement with the observations.

In the barogram we find pressure fluctuations throughout most of the day. They can be connected to gravity waves. Since the front passing Oppdal is aligned almost along the flow at the surface, the conditions with stable air near mountain top upstream can have lasted longer than in the other cases. We have not estimated the frontal passage for this case.

### 3.1.5. Case e 31.01.95

A low of 963 hPa is seen at about 64° N and 04 ° W in the surface map valid 06 UTC (Figure 4e). An occlusion and a warm front is crossing southern Norway from WSW. The Synop report from Oppdal at 18 UTC (Figure 5e) gives a past maximum wind force of 30 knots.

As the warm front approached Norway a low-level jet of about 35 m/s is found ahead of the front.

The cross-sections in Figure 6e and 7e valid 15 UTC reveals a sharp warm front with a marked inversion underneath. The wind maximum is now simulated at the lowest vertical level among the 5 cases.The maximum north of the mountain top is now above 50 m/s.

The simulated mountain waves are confined to the lower troposphere. The stability maximum around 700 hPa is pronounced. Above the stability is much lower. There is also a strong wind shear above the stable layer. Both these features contribute to a low Richardson number at the top of the stable layer.

Looking at the TEMPs we see that there are errors in both wind and temperature at Ørlandet.

Out of the five cases, case e has the most marked vertical variation in static stability. In addition, the wind shear contributes to conditions known to trap the gravity waves in the lower troposphere. The 50 km simulation gives a shallow layer with strong winds compared to the other cases. This gives us reason to believe that the need for better resolution of the mountains is large indeed. The case has been chosen for simulation with 10 km resolution. Results are given below.

The barogram shows pressure fluctuations throughout the day. The secondary minimum at 13 UTC we will connect to the passage of the front.

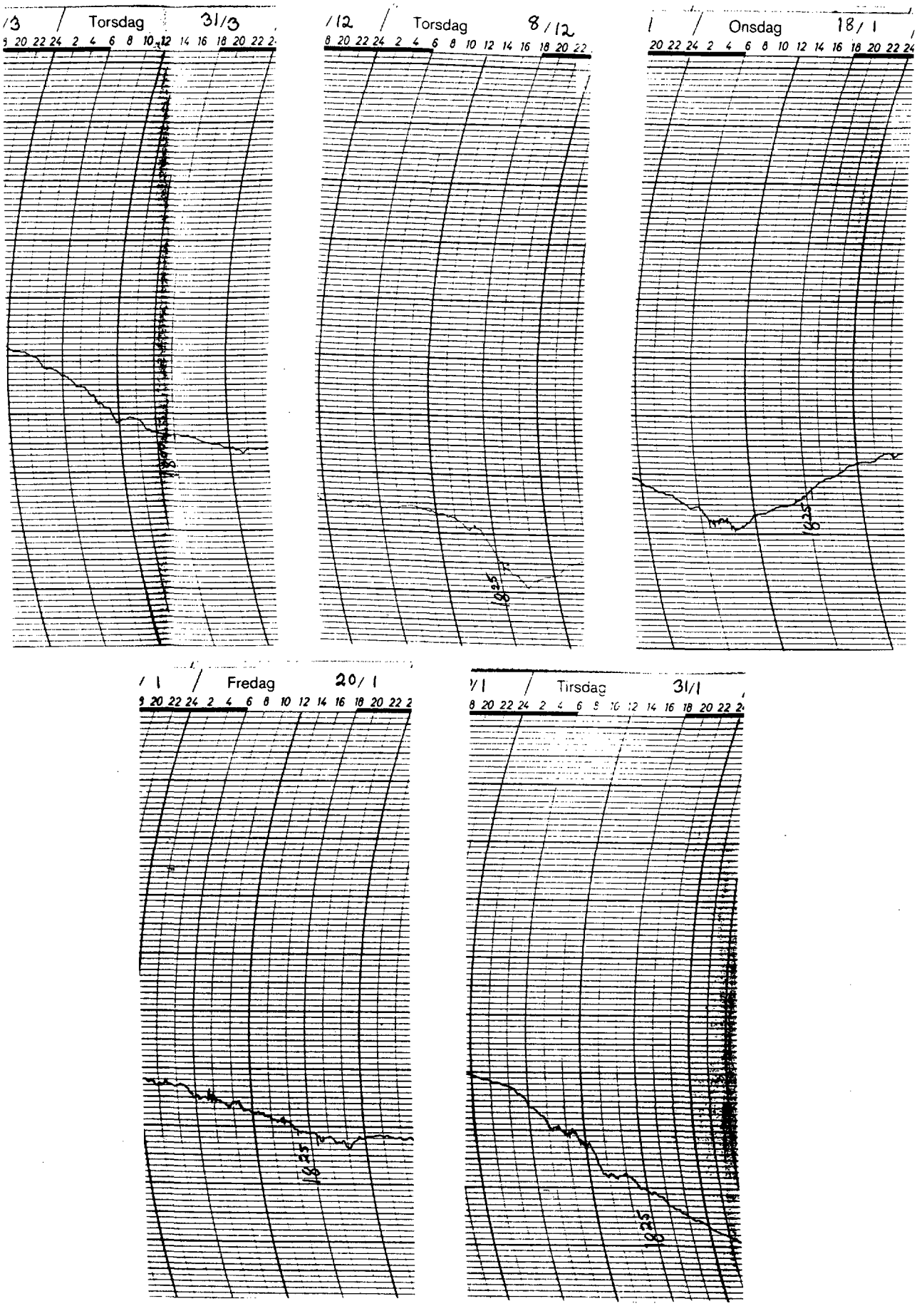


Figure 11. Pressure diagrams for Oppdal covering the five cases a-e. Date and time is at the top of the diagram. The time is local time (winter time) which is one hour ahead of UTC for all the five cases. The horizontal lines are for each hPa.

## 3.2 Simulation of case e with LAM10.

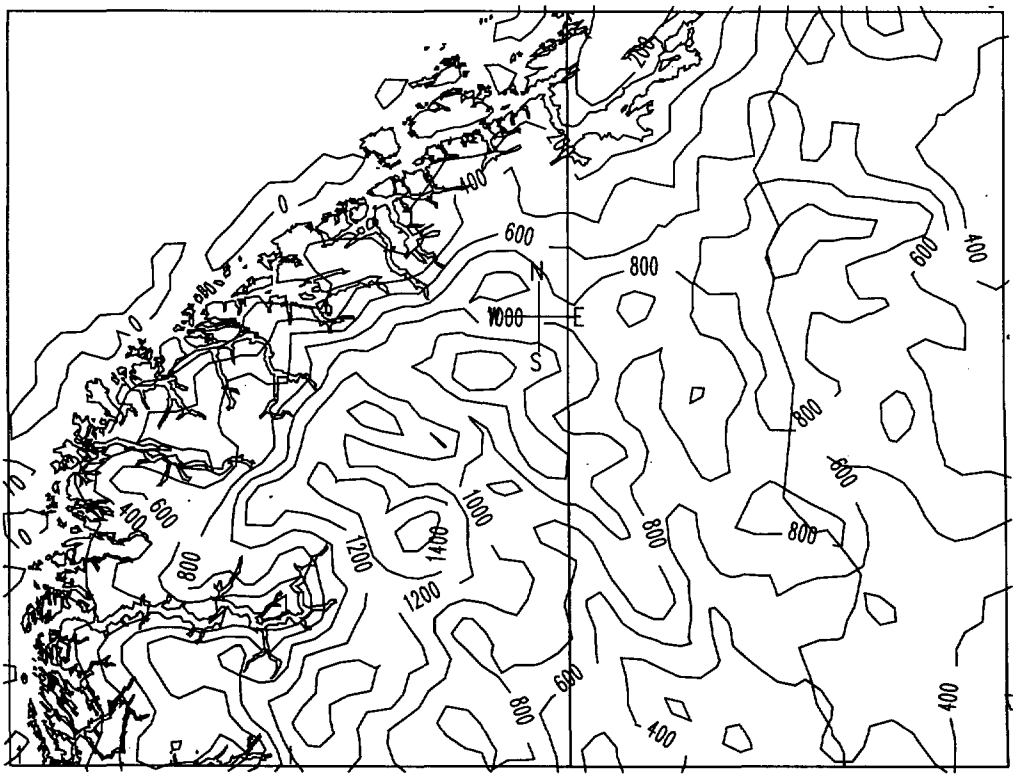


Figure 12.Model topography for LAM10. Isolines for every 200 m.

The model topography used for this experiment is shown in Figure 12. The Aa cross-section of the 10 km run (Figure 13) shows a much more detailed flow. A horizontal map of winds at model level 27 (near the maximum) is included in Figure 14. We see that the model resolves more than one single maximum of the topography of Southern Norway. The smallest details of the mountains downhill force gravity waves in the flow almost vertically aligned. Comparing with the 50 km cross-section, we see that the wind maximum aloft is retained (note that the arrows in the 10 km figure now gives tangential displacement in 6 minutes.). Going to the conditions at Ørlandet at 12 UTC (Figure 15), the improvement over the 50 km simulation is remarkable when looking at the wind. The simulated temperature profile also has more details although the vertical position of the details is a little wrong. Since the model is not in a steady state, it could be tempting to suggest a phase error in the gravity waves as a source for this error, since the simulated wind capture most of the observed variation in the vertical. Further investigations are, however, required before drawing conclusions on this last point.

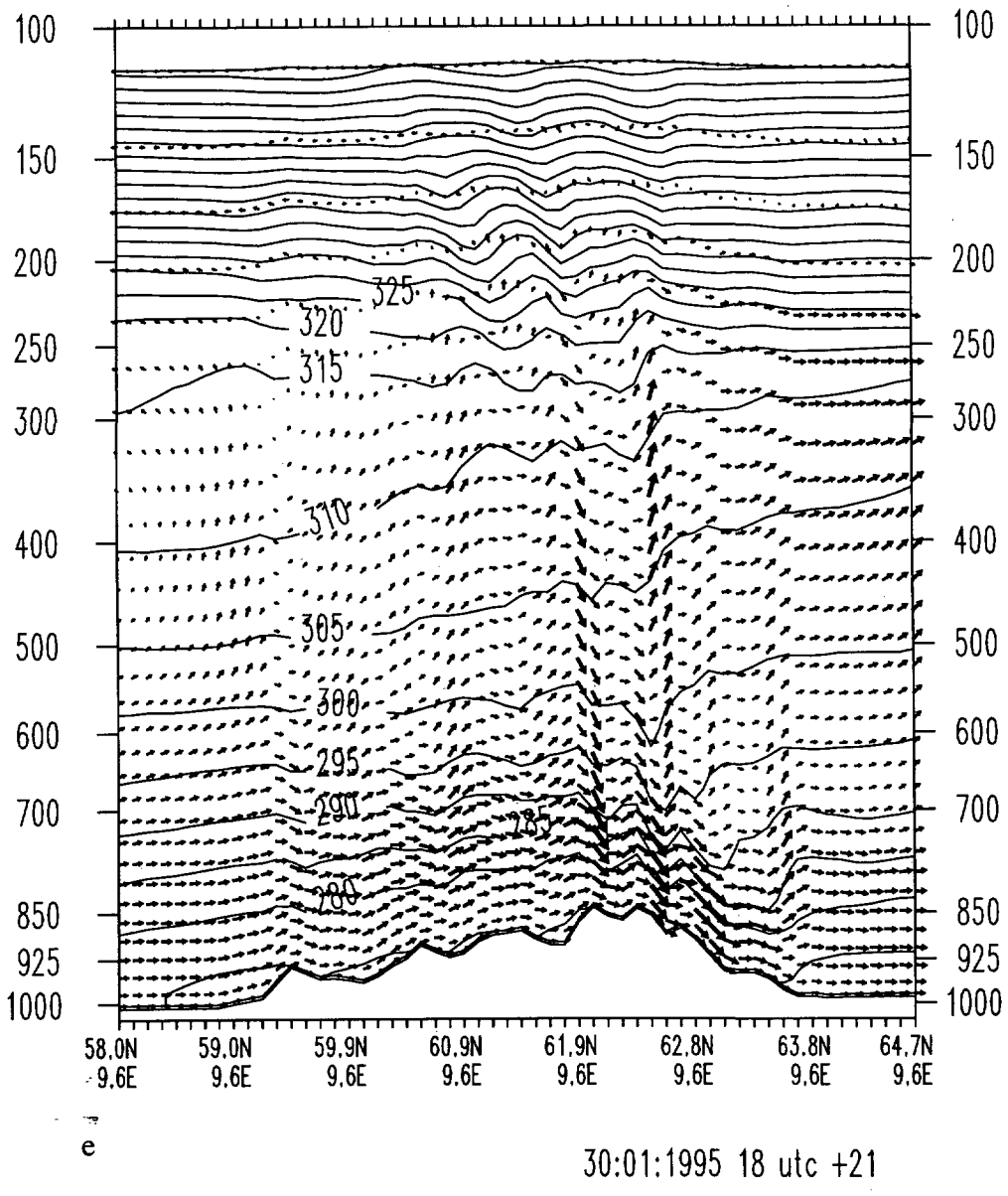


Figure 13. Cross section Aa from LAM10 for case e. Position of this cross section is displayed in figure 3. Vertical axis is pressure (hPa). Positions in degrees along the horizontal axis (decimal). Solid lines give potential temperature. Arrows give tangential displacement in 6 minutes. Decimal position of Oppdal is 62.60 N and 09.70 E.

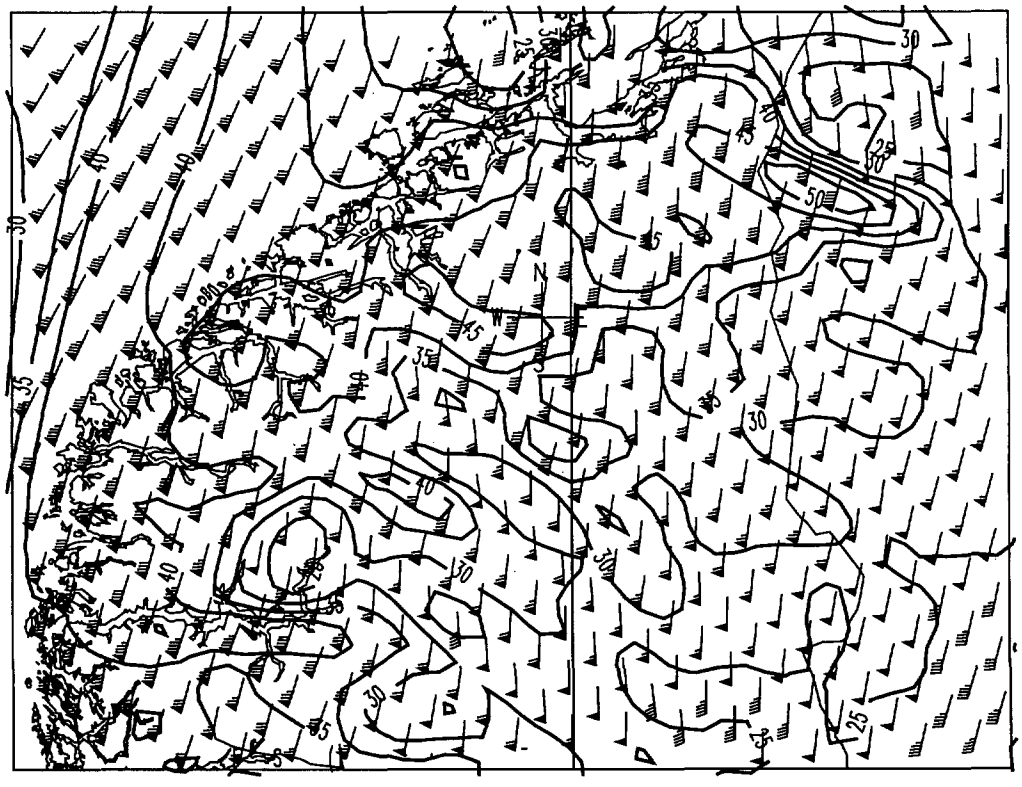

Figure 14. Maps of simulated wind in LAM10 model level 27 for case e (third arrows from the bottom in the cross-sections in Figure 15 is for the same level). Wind arrows for every second grid point (knots) and isolines of wind speed (m/s). A cross-(with direction letters S,E,N,W) marks the position of Oppdal

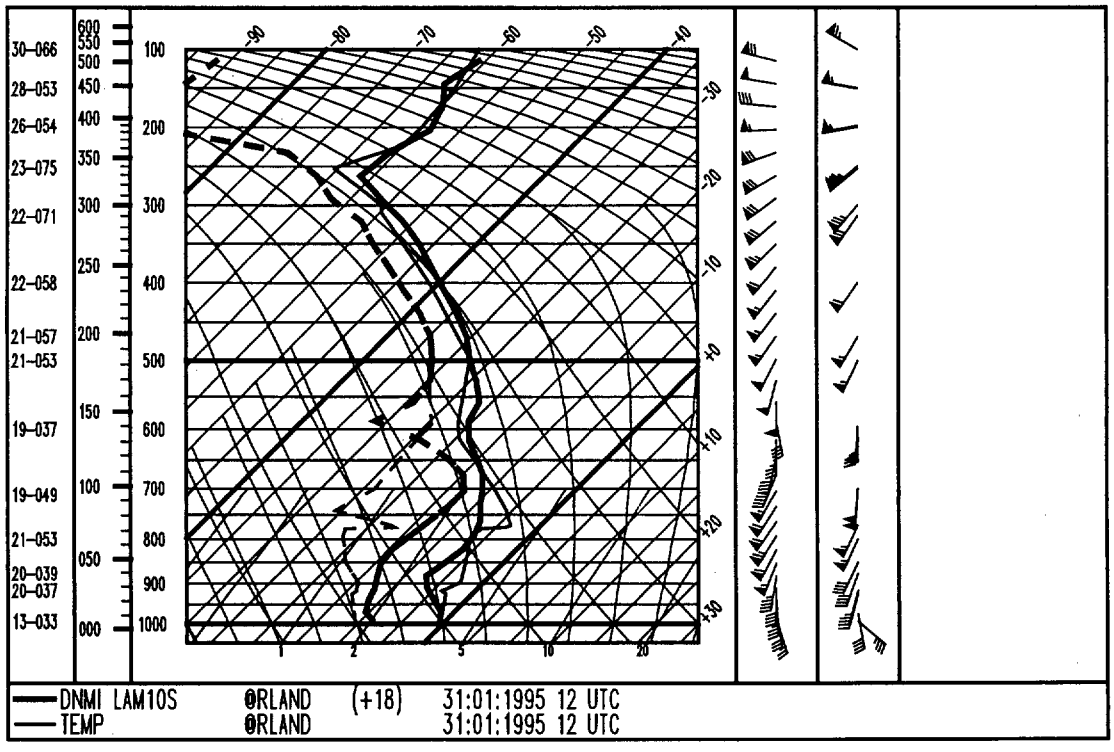


Figure 15. Simulated LAM10 vertical profile (thick lines)and observed vertical profiles(thin lines) of temperature and dew point at Ørlandet. The diagram is an Amble diagram which is a skew T, ln p diagram below 500 hPa and a skew T, p diagram above. Wind arrows for the simulated 30 levels and observations are given in two columns to the right in the figure. Some wind observations are for technical reasons plotted on top of each other. Selected observed winds are, however found as direction (tenths of degrees) and force (knots) in the left part of the figure.

## 4. Discussion

Verification against the available observations were presented in the previous section. In this section we will discuss all the cases and try to point at common features as well as differences.

In the introduction we mentioned the exsistence of several theories for downslope windstorms. According to Durran (1990) the simplified physics of the two dimensional hydraulic jump explain most aspects even of the more complicated atmospheric problem. A second theory is that some reflection is of gravity waves take place at the tropopause if the atmosphere is properly "tuned" in terms of upstream means values of velocity and static stability. The importance of tuning is discussed by Durran. For strong Boulder windstorms the tuning might be a necessary but not sufficient condition for strong cases. Durran points at the importance of an inversion near mountain top level. In our an inversion is seen at in the model simulation (Figure 9a). Above this layer there is a layer with lower stability. The case could therefore be covered by the third theory of downslope windstorms, namely the theory of a "critical layer". The critical layer has a low Richardson number and might act as an effective reflector of gravity wave energy downwards.

According to Durran, the theory of a critical layer identified by a low Richardson number above a more stable layer is a necessary for explaining the full physics of the problem. When investigating Boulder cases, Durran (1990) finds that the existence of an inversion near mountain top upstream is found in some strong windstorms. All our cases seem to bear the characteristics of a critical layer. The vertical variation of static stability is so that there are a more stable layer near mountain top level. In case b and e there is strong wind shear. Case e seems to be the most "pronounced" critical layer case as in this case we find both low stability and large wind shear above the marked stable layer. We conclude that for the five cases, a critical layer can probably be indicated in all the cases. In case b and c, however, the situation is most uncertain. A marked wind shear is present in case b, but the variation in the stability is small. For both cases the critical layer effect seems to be week and the reflection might have taken place at the tropopause. The Southern Norwegian mountains have comparable scales along and across the flow. The moving cyclones and the fronts beeing forced by the mountains, makes the spatial variations rather complex for all the cases. Indications of strong winds based on two dimensional parameters for defining a critical layer, seems nevertheless to apply to our cases, at least quantitatively.

The five windstorm events were connected to the frontal system of a moving synoptic scale cyclones. The damage seems to occur just before the front passes the Oppdal area. The five weather situations is different in terms of surface low track as well as synoptic scale frontal analysis. When the front is upstream of Southern Norway, we find as a common feature a warm front or an occluded front. Ahead of this front there is a more stable layer or even an inversion connected to the front (warmer air aloft) Out of the five cases, case e represents the most pronounced realization of this feature while case b is the weakest. Connected to the stable stratification there is a low-level wind maximum or a low-level jet just ahead of the front. The frontal analysis is more complicated as the front interacts with the mountains. The low-level wind maximum is now generally stronger. The warm front seem to be deformed by the mountain flow so that the stability is increased in the lower layers.

The synoptic scale surface pressure seems to be well simulated. The downstream sounding at Ørlandet reveals discrepancies in the vertical wind profiles for the cases b,c,d and e. The most pronounced differences are found in the cases wind a marked wind shear in the troposphere upstream, namely b and e. Nested simulation with 10 km grid did however remove the most severe errors for case e. Most of broader scale mountain flow of the 50 km run is still present in the 10 km run like the layering of the atmosphere and the wind maximum aloft near the Oppdal area.There is not evidence given the available observations that the 10 km simulation is not correct as far as the 10 km grid can resolve. It seems as if the hydrostatic model captured the main features of the flow over and around the mountains.

The local observation material is in fact so that we can not be sure that the strongest winds at Oppdal occur ahead of the passage of the surface front. There is, however, reasonable to suggest so as the conditions for a critical layer is found ahead of the front. Based on the simulations and the barograms we included our estimates of the frontal passage at Oppdal in section 3.

Our simulations do not describe breaking of gravity waves. The almost vertical simulated potential temperature contours downstream above the wind maximum is an indication of low static stability. This steepening of the contours is built by the gravity waves. In the atmosphere convective instability can be released in such areas and the wave breakes. The vertical acceleration can be so large that the assumption of hydrostacy breaks down. The model parameterization of vertical diffusion will avoid unstable conditions but the way it avoids the

release of convective instability is probably a main weakness in the simulation. The errors in the simulation of case a (discussed in section 3.1.1) can be caused by this effect since the vertical diffusion will not smooth the profile as effective as the atmosphere can do it by the processes described above. Small scale variations (fluctuations) in the observed pressure at Oppdal is seen in the barograms from case b,c,d and e. This feature might be a manifestation of a process connected to convective instability and breaking waves. Durran refers to Clark and Farly (1984) who suggest a competition between gravity wave build-up via forced gravity wave dynamics and wave breakdown via convective instability, producing fluctuations in wind and pressure. A very interesting point when we come to non-hydrostatic simulations in the future, is the possibility for reproducing such fluctuations.

If the grid is to be increased beyond 5 km, it is possible to resolve much steeper mountains. When steeper mountains are resolved, the flow might much more easy violate the hydrostatic assumptions and non-hydrostatic model is required.

We have above presented data from five numerical simulations. The cases were selected by windstorm damage in the Oppdal area. Since all the windstorm cases in a one year period were included, the cases should represent typical weather situation in which windstorms in Oppdal are experienced.The period of one year is, however, too short from a climatological point of view. In section 2 we discussed the local winds in Oppdal. Here we will only mention that damage at Oppdal as a criterion of windstorms in the area excludes cases when equally strong windstorms do not affect the community at Oppdal. This is because the area is sparsely populated. The largest areas are not populated at all. If the wind direction is a little different, the strongest winds may not be taken note of by anyone. It can of course, nevertheless, be interesting to investigate the circumstances for the event. An additional problem is that once the damage has occurred, the damaged construction can not be used as a strong wind indicator before eventually being rebuilt. In our investigation some common features for down slope windstorms at Oppdal are identified. To what extent those features are sufficient for strong cases remains to be seen.

## 5. Summary

Five windstorm cases were simulated with a 50 km resolution non-hydrostatic limited area model and compared to conventional observations. Synoptic scales were simulated well. Hydrostatic mountain waves were identified in the simulations. The 50 km model failed to simulate the vertical wind variation in two of the cases. A 10 km simulation of one of the latter cases captured most of the wind variation. The gravity waves were reflected in the troposhere and a wind maximum in a hydraulic-jump-like mountain wave were formed on the lee side of the mountain. The conditions for the local windstorms were connected to a layer of increased stability ahead of warm fronts or occlusions crossing and interacting with the Southern Norwegian mountains. The local data of the maximum winds and the time it occurred were sparse. Based on identification of a critical layer, we did, however, assume that the strongest winds occurred ahead of the surface front

## 6. References

Bratseth, A.M., 1986: Statistical interpolation by means of successive corrections. Tellus 38 A, 449-447.

Durran, D.R., 1990: Mountain waves and downslope winds. Atmospheric Processes over Complex Terrain. American Meteorological Society, 23, 59-81.

Grønås, S. and Hellevik, O., 1982: A limited area prediction model at the Norwegian Meteorological Institute. DNMI Technical Report No.61.

Grønås, S. and Midtbø, K.H., 1987: Operational Mulitivariate Analyses by Successive Corrections. Collection of Papers Presented at the WMO?IUGG NWP Symposium, Tokyo, 4-8 August 1986.

Neiman, P.J., R.M. Hardesty, M.A. Shapiro and R.E. Cupp, 1988: Doppler lidar observations of a downslope windstorm. Mon. Wea. Rev., 116, 2265-2275.

Nordeng, T. E., 1986: Parameterization of Physical Processes in a Three-Dimensional Numerical Weather Prediction Model. DNMI Technical Report No.65.

Smith, R. B., 1989: Hydrostatic airflow over mountains. Advances in Geophysics, Vol. 31,Academic Press, Inc.
23.6.95: